NATIONAL ADVISORY COMMITTEE FOR AERONAUTICS

WARTIME REPORT

ORIGINALLY ISSUED
September 1940 as
Advance Confidential Report

PRELIMINARY TESTS IN THE NACA TANK TO INVESTIGATE THE FUNDAMENTAL CHARACTERISTICS OF HYDROFOILS

By Kenneth E. Ward and Norman S. Land

Langley Memorial Aeronautical Laboratory
Langley Field, Va.

Wartime Report L-766, "Preliminary Tests in the NACA Tank to Investigate the Fundamental Characteristics of Hydrofoils," by Kenneth E. Ward and Norman S. Land was distributed along with a large number of other reports written during the war. A recent critical review of Wartime Report L-766 indicates that some of the hydrofoil data contained therein are invalid. The NACA therefore recommends that, instead of Wartime Report No. L-766, the two following papers, which contain the most accurate data available on the drag of hydrofoils at high water speeds, be used:

a. Wartime Report L-757 entitled "Characteristics of an NACA 66, S-209 Section Hydrofoil at Several Depths," by Norman S. Land.

b. Wartime Report L-758 entitled "An Investigation of Hydrofoils in the NACA Tank I - Effect of Dihedral and Depth of Submersion," by James M. Benson and Norman S. Land.

NATIONAL ADVISORY COMMITTEE FOR AERONAUTICS

PRELIMINARY TESTS IN THE NACA TANK TO INVESTIGATE THE FUNDAMENTAL CHARACTERISTICS OF HYDROFOILS

By Kenneth E. Ward and Norman S. Land

SUMMARY

The present preliminary investigation was made to study the hydrodynamic properties and general behavior of simple hydrofoils. Six 5- by 30-inch plain, rectangular hydrofoils were tested in the NACA tank at various speeds, angles of attack, and depths below the water surface. Two of the hydrofoils had sections representing the sections of commonly used airfoils, one had a section similar to one developed by Guidoni for use with hydrofoil-equipped seaplane floats, and three had sections designed to have constant chordwise pressure distributions at given values of the lift coefficient for the purpose of delaying the speed at which cavitation begins.

The experimental results are presented as curves of the lift and drag coefficients plotted against speed for the various angles of attack and depths for which the hydrofoils were tested. A number of derived curves are included for the purpose of better comparing the characteristics of the hydrofoils and to show the effects of depth. Several representative photographs show the development of cavitation on the upper surface of the hydrofoils.

The results indicate that properly designed hydrofoil sections will have excellent characteristics and that the speed at which cavitation occurs may be delayed to an appreciable extent by the use of suitable sections.

INTRODUCTION

A hydrofoil is, by definition, any surface designed to obtain reaction from the water through which it moves. One of the first to use hydrofoils was Forlanini in Italy in 1898 for the purpose of supporting high-speed boats on the water with a minimum amount of resisting force. A number of later developments were made by Crocco, Bell, and others for the same general purpose.

The first practical application of the use of hydrofoils to assist the take-off of a seaplane from the water was by Guidoni in Italy and his first successful flight was made in 1911. Guidoni conducted a comprehensive investigation of hydrofoils and of seaplanes equipped with hydrofoils. The SVA seaplane, developed by Guidoni in 1917, is perhaps the best known example of a seaplane having floats provided with hydrofoils.

There has been a recent revival of interest in hydrofoils, with particular respect to their use in assisting the take-off of long-range flying boats. The use of hydrofoils provides the possibility of a greatly improved aerodyhamic form for the flying boat with the resulting increase in performance in the air. Hydrofoils also are known to have good rough-water characteristics and their use may result in a substantial decrease in the structural weight of the hull.

There is a present need for fundamental studies regarding the properties of hydrofoils. The almost complete lack of design data has probably been a deterrent to the use of hydrofoils in modern applications. Any fundamental studies should include tests of hydrofoils of large sizes, mainly because of the scale effect on cavitation, in order to obtain reliable data regarding the most practical sections and arrangements to be used.

The present preliminary investigation was made to study the general behavior of simple hydrofoils. Six hydrofoils, rectangular in plan form and with constant sections, were tested in the NACA tank during November and December 1938. Five of these hydrofoils are similar to airfoils that have been tested in the NACA variable-density wind tunnel. The sixth represents, as nearly as feasible, one of the sections described by Guidoni in reference 5. They were suspended in the water below a balance secured to the towing carriage and the lift, drag, and pitching moment were measured at various speeds, angles, and depths of submersion.

APPARATUS AND TESTS

A description of the NACA tank and the towing carriage is given in reference 1. The balance, which is supported on the main structural members of the towing car-

riage, is shown diagrammatically in figure 1. It is designed to measure the lift, drag, and pitching moment of the hydrofoil. Basically the balance consists of a heavy floating frame connected by means of linkages to cantilever springs attached to the main frame, and to the regular resistance dynamometer of the carriage. The floating frame contains a movable unit including two struts and the hydrofoil which can be adjusted to change the angle of attack and the depth of submersion of the hydrofoil. The struts are tapered and have bi-convex sections with constant radii of 5-5/8 inches and sharp leading and trailing edges. They are spaced 16-1/8 inches between centers and are attached to the upper surface of the hydrofoil with the center line of the struts at the half-chord position on the hydrofoil. The chord of the strut at the attachment point is 2.9 inches. The chord line of the hydrofoil has an initial angle of attack of 6° when the struts are vertical. It is interesting to note that the spacing between struts of 16-1/8 inches, which was computed to give equal bending loads on each side of a strut, was found to be justified when one hydrofoil was accidentally overstressed and deformed during a test at high speeds.

The hydrofoils are all rectangular in plan form with square tips and constant sections. They have a chord of 5 inches and a span of 30 inches and, except for the Guidoni section which is steel, are machined from hard brass. The method of construction is the same as that described in reference 2 for construction of the airfoils tested in the variable-density wind tunnel and they are finished with the same degree of surface smoothness.

Six hydrofoils were tested in this preliminary investigation, two having sections commonly used for airfoils, one having a section developed by Guidoni, and three having sections designed for uniform chordwise pressure distributions. The profiles of these sections are shown in figure 2. The NACA 23012 (reference 3) was chosen as representing a commonly used airfoil section for which considerable data are available from wind-tunnel and free-flight tests. The NACA 23006-33 (0006-33 thickness distribution (reference 4) disposed on the 230 mean line (reference 3)) was chosen to represent a thin airfoil section having a small leading-edge radius.

The Guidoni represents a section used by Guidoni in a practical application. (See reference 5.) The ordinates for this section were determined from the illustra-

tion published in reference 5 and may not exactly duplicate the original section.

The sections for uniform chordwise pressure distributions are represented by the NACA 25 B 09-46, the NACA 16-509, and the NACA 16-1009. In choosing these sections, it was recognized that the cavitation phenomenon is associated with the low pressures developed on the lifting surface of the hydrofoil. Pressure-distribution investigations show that the usual airfoil shape results in a very irregular distribution along the chord. For all but the lowest values of the lift coefficient, sharp peak pressures develop near the leading edge due to very rapid acceleration of the air. Because of the association between the low pressures on the section of a hydrofoil and the development of cavitation, it was apparent that if a section could be developed which had a uniformly constant pressure along the chord, much higher normal forces could be obtained without reducing the pressure at any point below the vapor pressure of the water and thus causing cavitation of the flow. While investigating the shapes of sections which would give the desired distribution, it was found that such sections were being developed for high-speed airfoils. The NACA 25 B09-46 (reference 6) represents one of the earlier development forms. The NACA 16-509 and NACA 16-1009 are later sections developed as described in references 6 and 7 and subsequently tested in the 24-inch high-speed tunnel. These sections are designed to have a uniform chordwise pressure distribution at given values of the lift coefficient ($C_L = 0.5$ for the 16-509 and $C_L = 1.0$ for the 16-1009).

In making tests of the hydrofoils, the strut pivot is bolted in a position which places the hydrofoil at a chosen nominal depth and angle of attack. The carriage is then operated at constant speeds and the forces are observed throughout the range of speeds within the limits of the strength of the hydrofoil or of the apparatus. (Lift forces of over one ton per square foot were measured in the present investigation.) The speed at which cavitation first appears is noted and representative photographs of the phenomenon are taken. The procedure is repeated for various angles of attack and for various nominal depths. The temperature and level of the water in the tank are determined for each test.

RESULTS

Experimental results.- The experimental results are presented as curves of lift and drag coefficients plotted against speed in figures 3 to 8. Each set of curves shows the variations of the coefficients with change in speed for constant values of the angle of attack and for several representative depths of submersion. The forces are reduced to coefficients of the usual aerodynamic form,

$$\text{Lift coefficient} \quad C_L = L / 1/2\ \rho_w\ V^2\ S$$

$$\text{Drag coefficient} \quad C_D = D / 1/2\ \rho_w\ V^2\ S$$

where L total lift force, lb

D drag force, lb

ρ_w mass density of water, 1.968 slugs/cu ft for these tests

V speed, fps

S area of hydrofoil, sq ft

The drag coefficient is based on the total drag of the hydrofoil and strut system which is submerged. Windage corrections have been applied for the balance and that portion of the struts above the water line. These corrections were determined by measuring the forces using sections of dummy struts on the balance running just clear of the water surface.

Pitching moments are not included in the results because the sensitivity and operation of the balance were not sufficiently good to give consistent and reliable data for the moments. In practical applications the pitching moment of the hydrofoil will be negligible compared with the moments resulting from the lift and drag forces.

Speeds are presented in dimensional units because it is not considered feasible at the present time to establish a nondimensional form. In high-speed airfoil work the speed of sound, which represents the rate at which pressures are propagated through the fluid, provides a convenient value upon which to base a nondimensional speed ratio. In working with hydrofoils, a logical choice for

a similar ratio would probably be the speed at which cavitation begins. This speed is mainly a function of the vapor pressure of the fluid, and the minimum pressure developed by the hydrofoil which is a function of the size, shape, and attitude of the section. It is possible that, with further study, a satisfactory method of determining a cavitation speed may be found and this speed used to give a nondimensional ratio of speeds which may have some advantage over the dimensional quantities. For those interested in using the Reynolds number in connection with the present results, the value of the kinematic viscosity of the water in the tank may be found from the empirical relation

$$\nu = (20{,}700 + 875t + 2\,t^2)^{-1} \text{ ft}^2/\text{sec}$$

where t is the temperature of the water in degrees Fahrenheit.

The depth of submergence of the hydrofoil is generally given in the results as the nominal depth d of the quarter-chord of the section in terms of the chord c. The nominal depth represents a fixed position of the pivot on the balance and differs from the actual depth because of the angular change and the small daily variation in the water level. The actual depth is of importance only when the hydrofoil is near the surface because of the relatively small changes in the hydrofoil characteristics with dpeths below two chords. The actual depth may be readily obtained for any specific requirement from the relation

$$d/c = 6.42 \cos(\alpha - 3.7^\circ) - k$$

where d/c actual depth of quarter-chord point in terms of the chord

α angle of attack, degrees

k trim, including the nominal depth, water level, and correction for the thickness of the hydrofoil (values of k are included with the figures)

The results are given for nominal depths of 1c, 2c, and 5c for all of the hydrofoils tested and, in addition, the results for a nominal depth of 1/4c are included for the NACA 23012 and the Guidoni. Some tests were made for

a nominal depth of 3c, but the results are not included because they differ so little from the results obtained for the depths of 5c.

The speed at which cavitation begins, V_C, is indicated by small arrows on the curves. These speeds represent the speeds at which cavitation first appeared on the upper surface of the hydrofoil. There was some evidence of cavitation on the lower surface of the hydrofoil, at low values of the angle of attack, from observations of the wake behind the hydrofoil, but the speeds at which it first appeared were not recorded.

Derived results.- Several series of curves are derived from the experimental results and are given in figures 9 to 17. The first series of curves (figs. 9 to 14) show the variations of the drag coefficient, lift-drag ratio, and cavitation speed, which are plotted against lift coefficient with speed as the parameter. These curves are given for two representative depths, 1c and 5c.

The effect of depth is shown in figures 15 and 16. Only the results for the NACA 23012 are given because these data are the most complete. The curves of lift and drag coefficients plotted against depth (fig. 15) are derived from the data given in figure 3, using the straight part of the curve, extrapolated where necessary. The drag coefficient and the angle of attack are plotted against the lift coefficient in figure 16 and compare these characteristics for four different depths. The drag coefficient C_D in this figure is based on the drag of the hydrofoil less the drag of the struts. Included in the figure are corresponding curves for a similar NACA 23012 airfoil. The curves for the airfoil were obtained from the data published in reference 8 and corrected to aspect ratio 6 by the usual method. All of the curves of figure 16 are given for a Reynolds number of 654,000 corresponding to a speed of 20 fps in the tank.

The drag of the struts was obtained from tests of the struts with the hydrofoil removed and does not take into account the interference effects. The drag coefficient for the submerged portion of the struts, based on the area of the hydrofoil, may be expressed by the relation

$$C_{D_S} = 0.0033 \ (d/c)$$

This relation is independent of the angle of attack, within the limits of accuracy of the tests, and holds for speeds below 50 fps at which speed the struts begin to cavitate when attached to the hydrofoil. It is interesting to note that the struts cavitated much later when tested without the hydrofoil and that the drag of the struts increased considerably when cavitation occurred. Corresponding measurements of the lift of the struts showed small, inconsistent values which are considered negligible within the limits of accuracy of the tests.

A comparison between the observed speeds at which cavitation began on the NACA 23012 hydrofoil and computed speeds based on the pressure distribution (obtained from wind-tunnel results by the methods of references 12 and 13) is shown in figure 17.

Several representative photographs showing the cavitation on the hydrofoil are given in figure 18. In taking these photographs, a strong light was placed above the surface of the water and the reflections were eliminated by the use of a polaroid filter in front of the camera lens.

Accuracy.- The accuracy of the experimental results, for an individual test, is indicated by the scattering of the test points on the curves. Check tests of the same hydrofoil, however, showed appreciable differences beyond the cavitation speeds with reasonably good checks at lower speeds. The later tests indicated that the drag was generally higher and the lift was inconsistently higher or lower than for the original test. The reasons for these differences are as yet unexplainable. It appears probable that small differences in the alinement of the balance may have caused the differences in the results. Every effort was made to keep the balance in proper alinement and to keep all operating conditions as nearly the same as practicable during the investigation. Another possible cause of the differences in the results may be due to a critical nature of the flow after cavitation has developed. The results as presented in this report are believed to be the most reliable of those obtained and give the correct order of the forces.

The speeds for each test point were accurately measured by the usual method of recording the time and distance for tests in the NACA tank. The speeds at which cavitation first appeared are probably a little high because of the

method and difficulty of observation. Check observations of the cavitation speed during the same test, however, agreed very closely. The observed values are believed to be correct within +5 and -0 fps.

The depths of the hydrofoils were accurately measured with respect to the still-water level at the beginning of each day of testing. A small reduction in water level occurred while a test was in progress through leakage of water from the tank but this reduction is considered negligible. Other sources of error are a constant depression of the water level under the carriage of about 1/8 inch caused by the pressure field around the moving carriage, and an irregular surge of the water in the tank of from zero to ± 3/8 inch.

There was no accurate control for setting the angle of attack of the hydrofoil and small errors were introduced from deflections of the balance structure under load. The probable limits of accuracy are believed to be within +0.2° and -0.3°.

DISCUSSION

Hydrofoil Characteristics

Experimental results.- The experimental results (figs. 3 to 8) in general show marked changes in the values of the coefficients with change in speed for constant angles of attack. Also, the different types of sections show considerable differences. The cavitation phenomena apparently have the largest effect, particularly for the hydrofoils having the usual airfoil sections. With the exception of some of the variations of drag, the usually smooth curves indicate that there are no sudden changes in the forces resulting from cavitation. The general shapes of the curves for any one hydrofoil are unaffected by the depth of the hydrofoil below the water surface, as may be seen by comparing the curves for different depths.

An interesting feature of the variation of the lift coefficient is the apparent approach to a limiting envelope which corresponds to a constant value of the total lift force as illustrated by the curves of figure 3d. This tendency is even more pronounced in the curves of some of the other figures. A possible explanation may be

in a limiting value for the change in momentum of the fluid acted on by the hydrofoil, owing to cavitation or other causes.

The hydrofoils having sections of the usual airfoil type (figs. 3 and 4) show the closest relation between the cavitation speed and the departure of the force coefficients from constant values. For these hydrofoils the lift coefficient decreases and the drag coefficient increases near the cavitation speed. The decrease in lift coefficient is relatively small but, at high angles of attack, the increase in drag coefficient is quite large.

The hydrofoils having sections designed for reduced cavitation (figs. 5 to 7) are of particular interest when operating near the design value of the lift coefficient. For these hydrofoils the lift coefficient falls off with increase in speed, at constant angles of attack, as for the other hydrofoils, but there was a large reduction in the drag coefficient to a minimum value which is apparently independent of the cavitation speed. This reduction in the drag coefficient with increase in speed is comparable with the results given in reference 6 where similar characteristics were found from tests of airfoils of this type. When the hydrofoils are operating at angles of attack above that giving the design value of the lift coefficient, the lift and drag coefficients both increase, with increase in speed, to a maximum and then decrease quite rapidly.

The increase in lift coefficient is probably due to a deformation in the effective profile of the section caused by separation in the cavitating area which results in an increase in the effective camber. This is one conclusion reached by Walchner (reference 10).

The Guidoni hydrofoil (fig. 8) shows the same general characteristics as the hydrofoils specially designed for reduced cavitation. It is of interest to note that the Guidoni sections, developed so many years ago, are still practical sections having good characteristics. The Guidoni sections are generally thin, however, with corresponding limitations in the load-carrying ability. The sections developed by the NACA are much thicker and permit a reduction in the number of supporting struts required for a given installation. Further tests are required to investigate the effects of a sharp or slightly rounded leading edge. Some brief qualitative tests indicate that

the small leading-edge radii of the NACA sections are satisfactory for breaking the water surface when a set of hydrofoils having dihedral emerges, as for a practical installation.

Derived results.- The curves of drag coefficients and lift-drag ratios (figs. 9 to 14) are useful for comparing the characteristics given by the different sections for equal values of the lift coefficient. These curves are dependent on the fairing of the basic curves but show the relative orders of the results. The curves for the usual airfoil sections (figs. 9 and 10) fall within reasonably uniform envelopes, with the individual curve for a given speed leaving the envelope when cavitation occurs. The variations of the drag coefficient and the lift-drag ratio with change in lift coefficient are about normal for the envelope curves when compared with similar results from wind-tunnel tests.

The corresponding curves for the hydrofoils having the other sections (figs. 11 to 14) show considerable differences in the variations for the different speeds, as might be expected from the differences shown by the original curves. The curves for the NACA 16-509 hydrofoil shown in figure 12a, best illustrate the variations for the sections designed for reduced cavitation. As the speed increases, the minimum drag coefficient is reduced and comes at higher values of the lift coefficient. The low values of the drag coefficient result in high values of the lift-drag ratio in the useful range of lift coefficients. Practical limits of testing unfortunately prevent the extension of all of the curves to give more complete information as to the general behavior of these hydrofoils at high speeds.

The general effect of depth of submergence of a hydrofoil is to decrease the lift and drag coefficients with decrease in depth. This effect is illustrated by the curves of figure 15 for a typical example. These curves represent the values of the coefficients before cavitation has disturbed the normal flow and show, in particular, the loss of lift as the hydrofoil approaches the surface. The corresponding values of the lift-drag ratio increase to maximum values when the hydrofoil is near the surface then decrease rapidly with further decrease in depth to values for planing surfaces.

The largest part of the change in drag coefficient

with change in depth is that due to the differences in the immersed lengths of the struts as may be seen by comparing the slopes of the curves with the value 0.0033 for the struts alone. When the hydrofoil approaches the surface of the water, the variation of both the drag and the lift coefficients with depth are affected by the large surface disturbance. This surface disturbance gives a decrease in actual depth over that determined with respect to the undisturbed surface, particularly for high angles of attack. An interesting observation is the large trough and high roach resulting from the downwash behind a hydrofoil operating near the surface.

The curves of angle of attack and drag coefficient for the NACA 23012 hydrofoil (fig. 16) show the relation between these characteristics for the hydrofoil at several depths, and the corresponding characteristics of a similar airfoil which was tested in a wind tunnel. The curves for the hydrofoil are derived from the curves of figure 15 for constant actual depths of the quarter-chord. The drag coefficient C_D represents the drag of the hydrofoil without struts in order to show better the comparison with the corresponding characteristics of the airfoil.

Inspection of the curves shows that, for the greatest depth, the characteristics of the hydrofoil are very similar to those of the airfoil. The almost constant differences in the drag curves are probably due to excessive values of the strut drag which may be too large because of the end interference in the tests of the struts alone. The slope of the curve of angle of attack, which represents the slope of the lift curve, is slightly greater than the corresponding slope for the airfoil over part of the curve. The slopes are not uniform, however, and tend to vary with change in lift in very much the same way that the slopes vary for most airfoils at low values of the Reynolds number. (See reference 8.) It should be remembered that these curves for the hydrofoil have been refaired from previously faired curves and that the data for the airfoil were obtained from interpolating between the curves of small-size figures. It is believed, however, that the curves as shown in figure 16 represent the correct orders of the characteristics.

An interesting feature shown in figure 16 is the apparent decrease in the effective aspect ratio of the hydrofoil with decrease in depth as indicated by the changes in slopes of the curves with change in depth. Also, the angle

of zero lift is increased with a decrease in depth. A possible explanation of these effects is that, as the hydrofoil approaches the surface, the spanwise lift distribution is changed, principally by a reduction of lift over the central portion of the hydrofoil. This would tend to reduce the effective aspect ratio and also would tend to require higher geometrical angles of attack for zero lift to compensate for the loss of lift of the central sections which, for the rectangular hydrofoil having constant and parallel sections, normally operate at a small positive lift when the total lift of the hydrofoil is zero.

Cavitation Phenomena

The phenomena of cavitation have been ably discussed, both from the theoretical and the experimental standpoints, by a number of authors. Ackeret (reference 9), Walchner (reference 10), and Smith (reference 11) have published papers of particular interest on the subject of cavitation.

Cavitation is a vaporization process resulting from a decrease in pressure in a fluid flow until the saturation pressure of the vapor is reached. It is a complicated polytropic process involving a very short time element. The analogy between cavitation and the compressibility phenomena of compressible fluids has been discussed by Ackeret (reference 9) in an extensive treatment of the subject. He shows that a shock occurs with the collapse of the bubbles and that there is a very rapid oscillation of the shock zone. The collapse of the bubbles of vapor in the shock zone produces impacts of the fluid on the bounding walls at extremely high velocities and hence enormously high pressures to which cause Ackeret attributes the erosion resulting from cavitation.

In the present investigation, the cavitation phenomena were studied only to the extent of observations of the nature of the cavitation as it appeared on the upper surface of the hydrofoil and of the speed at which it first appeared as a white fuzz or as streaks. Curves of this observed cavitation speed V_C are shown for all of the hydrofoils in figures 9 to 14. (Values of V_C are also indicated by small arrows on the curves of the experimental results in figs. 3 to 8.) The general characteristic of the curves of V_C plotted against C_L is a sharp de-

crease in the cavitation speed with increase in the lift coefficient. This characteristic is to be expected from considerations of the chordwise pressure distribution over the sections. For the sections designed for reduced cavitation, the curves show that the cavitation speed is delayed considerably at the lower values of the lift coefficient. The NACA 16-1009 hydrofoil gave the highest values of the cavitation speed over the greater part of the range of lift coefficients tested.

It was considered of interest to compare the observed values of the cavitation speed with the values computed from puressure-distribution diagrams. The NACA 23012 hydrofoil was chosen for this comparison because the data are the most consistent. The cavitation speed is computed on the basis of two simplifying assumptions: (1) that a cavity forms in the fluid at the surface of the hydrofoil when the absolute pressure at that point is equal to the vapor pressure of the water, and (2) that the pressure distribution on a hydrofoil is similar to that on the same section operating in air. Pressure distributions on airfoil sections are available from wind-tunnel measurements, or may be computed as in references 12 and 13. Either of these sources gives the pressures normal to the surface in terms of a nondimensional coefficient that is the ratio of the normal pressure to the dynamic pressure of the free stream. In aerodynamic work the coefficient has a negative sign where the normal pressure is less than the static pressure. The absolute value of the normal pressure is, of course, a positive quantity; so in this analysis the conventional aerodynamic pressure coefficient is preceded by a negative sign. Then by the first assumption:

$$p_v + p_{min} = p_a + p_w$$

where

p_v vapor pressure of water, lb/ft^2

p_{min} minimum normal pressure on surface of hydrofoil, lb/ft^2

p_a atmospheric pressure, lb/ft^2

p_w hydrostatic head at depth of point of minimum pressure, lb/ft^2

The value of p_{min} may be replaced by one in terms of the coefficient from the relations:

$$-P_{min} = p_{min}/q$$

and

$$p_{min} = -P_{min}\, q$$

where

P_{min} pressure coefficient at point of minimum pressure

$q = 1/2\ \rho_w\ V_c^2$ dynamic pressure, lb/ft^2

ρ_w mass density of water, $slugs/ft^3$

V_c speed at which cavitation begins, ft/sec.

Making the substitution and solving for V_c:

$$V_c^2 = \frac{p_a + p_w - p_v}{-P_{min}\ \frac{\rho_w}{2}}$$

For the 5-inch-chord hydrofoils tested, using the data as to the vapor pressure at the temperature of the water during the tests, and standard atmospheric pressure, the above expression reduces to:

$$V_c^2 = \frac{2120 - 27\ d/c}{-P_{min}}$$

where d/c is the depth-chord ratio. The value of P_{min} is determined for the midsection of the hydrofoil, assuming that the section lift coefficient c_l is equal to $1.14\ C_L$.

The results of this comparison are given in figure 17 and show very good agreement for the chosen example when consideration is given to the limitations of the method. The computed cavitation speed does not consider the preliminary stage of cavitation where dissolved gases are released from the liquid. Other factors are also neglected, such as the heat transfer, surface tension, etc. The diagrams of the pressure distribution are not exact for the

section considered and it is particularly difficult to judge the value of the minimum pressure coefficient because of the sharpness of the pressure peak. Furthermore, the values of the observed cavitation speed were difficult to obtain, particularly at high speeds, because of the limitations in the method of observation. The results, however, indicate that conservative values of the cavitation speed may be estimated by the method described.

The photographs of figure 18 show two distinct forms of cavitation. One form appears as streaks developing from point sources on the surface of the hydrofoil. There is no apparent reason for these sources as the surface of the hydrofoil was perfectly smooth to the touch and close examination did not reveal any protuberances nor discontinuities. The point sources do not appear consistently in the same places for different test runs and, with increase in speed, more of the sources appear until general cavitation over the whole surface takes place.

A second form of cavitation appears as a light, smooth haze uniformly distributed over a narrow band in the spanwise direction. This cavitation area follows the general picture of the pressure distribution and develops at a point along the chord where the minimum pressure is expected. The uniform spanwise distribution is interfered with by the presence of the struts as may be seen in some of the photographs. The pressure field around the struts is evidently sufficient to delay cavitation except at the intersection between the strut and the surface of the hydrofoil where local cavitation occurs.

Of special interest is the form of cavitation which develops on the surface of a hydrofoil designed for reduced cavitation. At values of the lift coefficient near that for which the hydrofoil was designed to have a uniform chordwise pressure distribution, the cavitation begins as a very thin, light haze well distributed over the central area of the hydrofoil. It has the appearance of a viscous fluid on the surface of the hydrofoil with large, slow-moving eddies on each side such as might be expected inside the boundary layer. With further increase in speed, the usual heavy, flame-like cavitation develops which is accompanied by severe vibration and noise.

Cavitation of the struts generally begins at the intersection with the surface of the hydrofoil at speeds between 50 and 55 fps. At higher speeds, general cavita-

tion of the struts takes place over the entire submerged length.

In many of the photographs, the tip votices plainly appear. It was interesting during the tests to observe these vortices, which are filled with a white mixture of water vapor and air, and note their behavior as they curled over the tips of the hydrofoil and expanded far downstream, until they were no longer visible. As the hydrofoil approached the surface of the water, the tip vortices would break the surface as they expanded and would form a wake pattern on the water corresponding with the popular conception of the vortex sheet behind an airfoil.

CONCLUDING REMARKS

The results of the present investigation indicate that properly designed hydrofoil sections will have excellent characteristics and that the speed at which cavitation occurs may be delayed to an appreciable extent by the use of these sections. Further work will include tests of practical arrangements and will cover the effects of dihedral, plan form, and multiplanes.

Langley Memorial Aeronautical Laboratory,
National Advisory Committee for Aeronautics,
Langley Field, Va.

REFERENCES

1. Truscott, Starr: The Enlarged N.A.C.A. Tank, and Some of Its Work. NACA TM No. 918, 1939.

2. Jacobs, Eastman N., and Abbott, Ira H.: The N.A.C.A. Variable-Density Wind Tunnel. NACA Rep. No. 416, 1932.

3. Jacobs, Eastman N., and Pinkerton, Robert M.: Tests in the Variable-Density Wind Tunnel of Related Airfoils Having the Maximum Camber Unusually Far Forward. NACA Rep. No. 537, 1935.

4. Stack, John, and von Doenhoff, Albert E.: Tests of 16 Related Airfoils at High Speeds. NACA Rep. No. 492, 1934.

5. Guidoni, A.: Seaplanes - Fifteen Years of National Aviation. Jour. R.A.S., vol. XXXII, no. 205, Jan. 1928, pp. 25-64.

6. Jacobs, Eastman N.: Preliminary Report on Laminar-Flow Airfoils and New Methods Adopted for Airfoil and Boundary-Layer Investigations. NACA ACR, June 1939.

7. Stack, John: Tests of Airfoils Designed to Delay the Compressibility Burble. NACA Rep. No. 763, 1943.

8. Jacobs, Eastman N., and Sherman, Albert: Airfoil Section Characteristics as Affected by Variations of the Reynolds Number. NACA Rep. No. 586, 1937.

9. Ackeret, J.: Experimental and Theoretical Investigations of Cavitation in Water. NACA TM No. 1078, 1945.

10. Walchner, O.: Profile Measurements during Cavitation. NACA TM No. 1060, 1944.

11. Smith, Lybrand P.: Cavitation on Marine Propellers. Trans. A.S.M.E., vol. 59, no. 5, July 1937, pp. 409-431.

12. Jacobs, Eastman N., and Rhode, R. V.: Airfoil Section Characteristics as Applied to the Prediction of Air Forces and Their Distribution on Wings. NACA Rep. No. 631, 1938.

13. Allen, H. Julian: A Simplified Method for the Calculation of Airfoil Pressure Distribution. NACA TN No. 708, 1939.

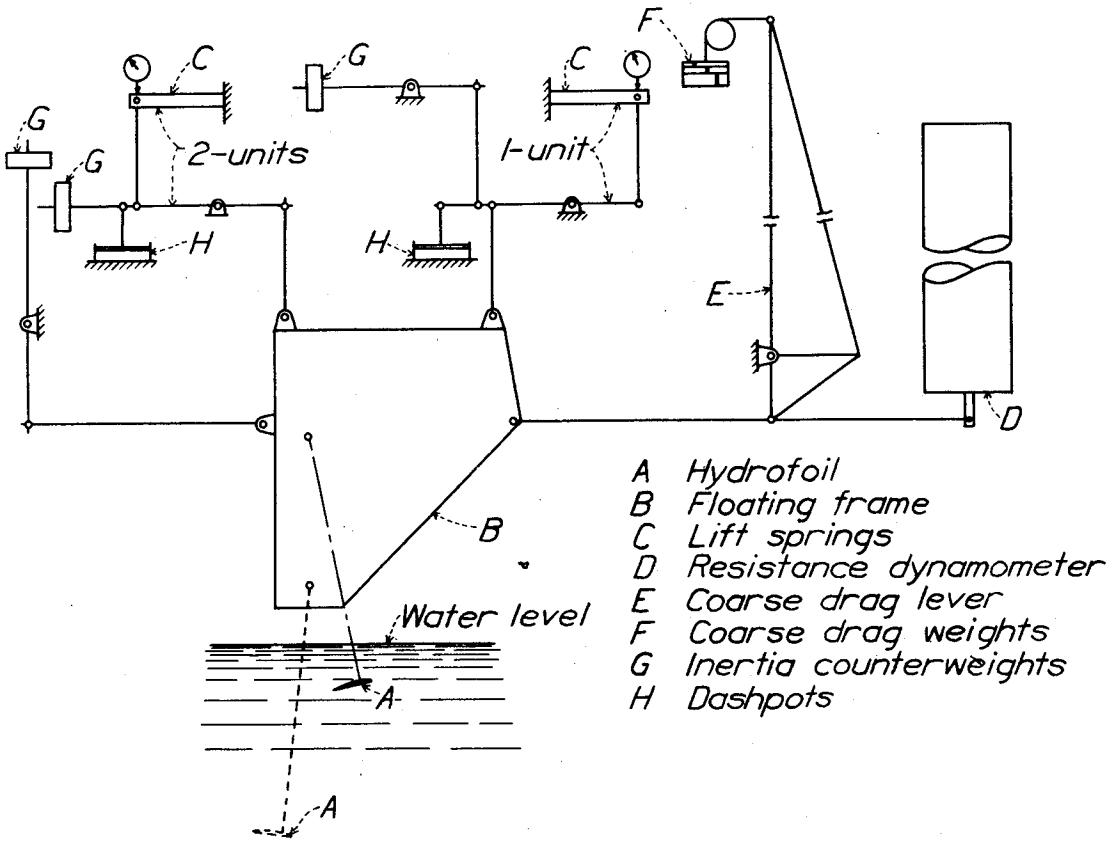

Figure 1.- Diagramatic sketch of hydrofoil balance.

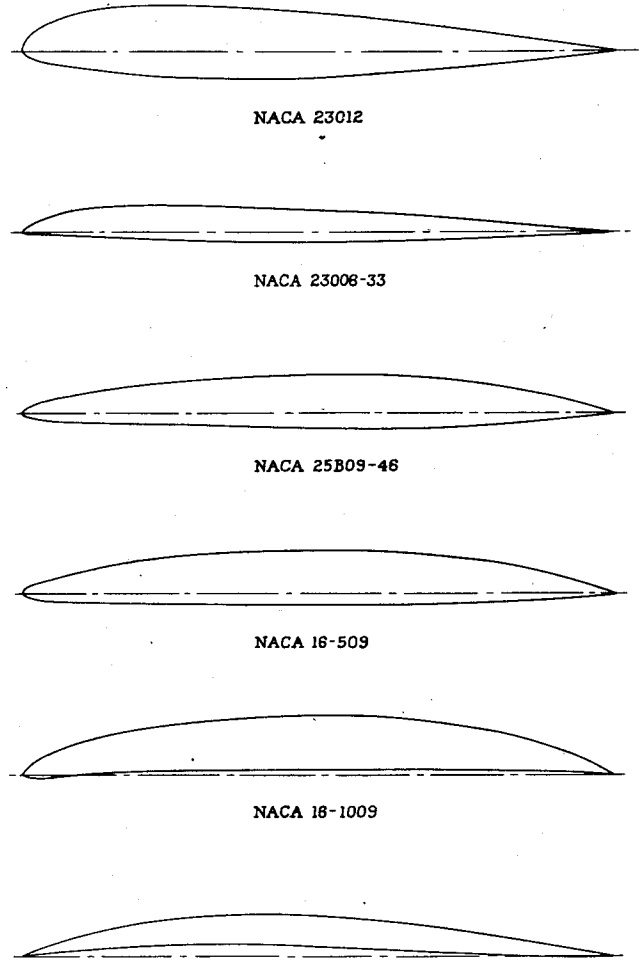

Figure 2.- Profiles of NACA hydrofoils.

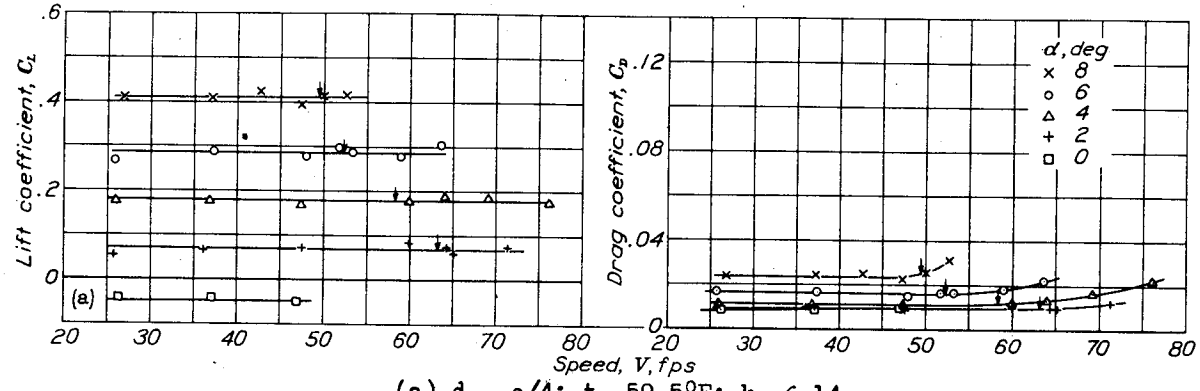

(a) d_o, c/4; t, 59.5°F; k, 6.14

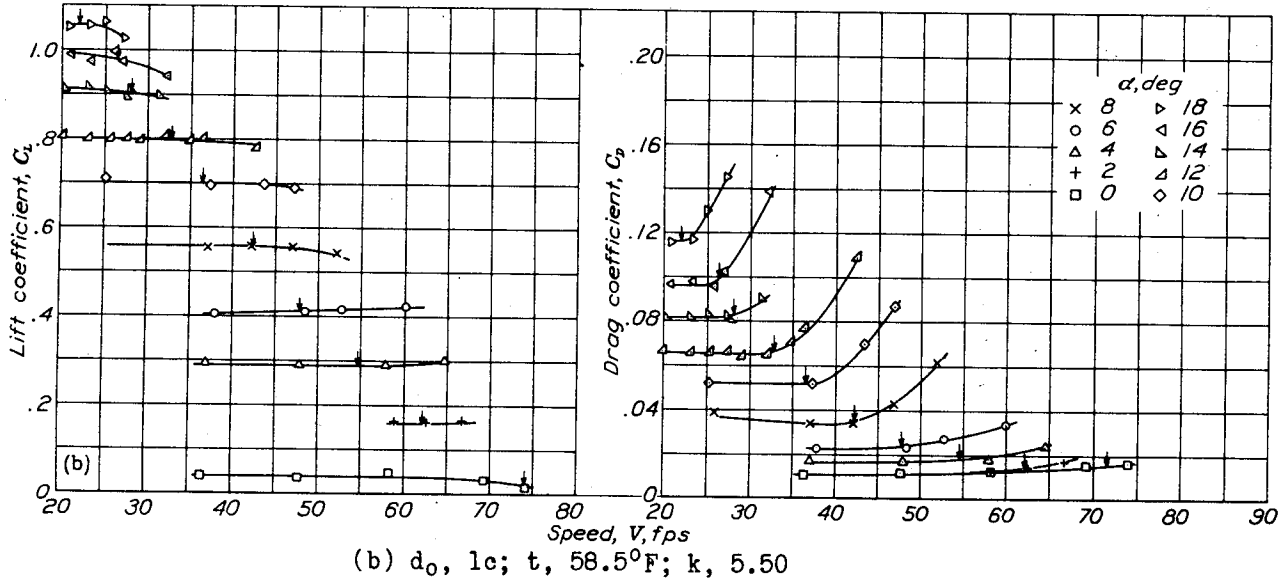

(b) d_o, lc; t, 58.5°F; k, 5.50

Figure 3a to d.- NACA 23012 hydrofoil. Variation of C_L and C_D with V.

(c) d_o, 2c; t, 59.5°F; k, 4.13

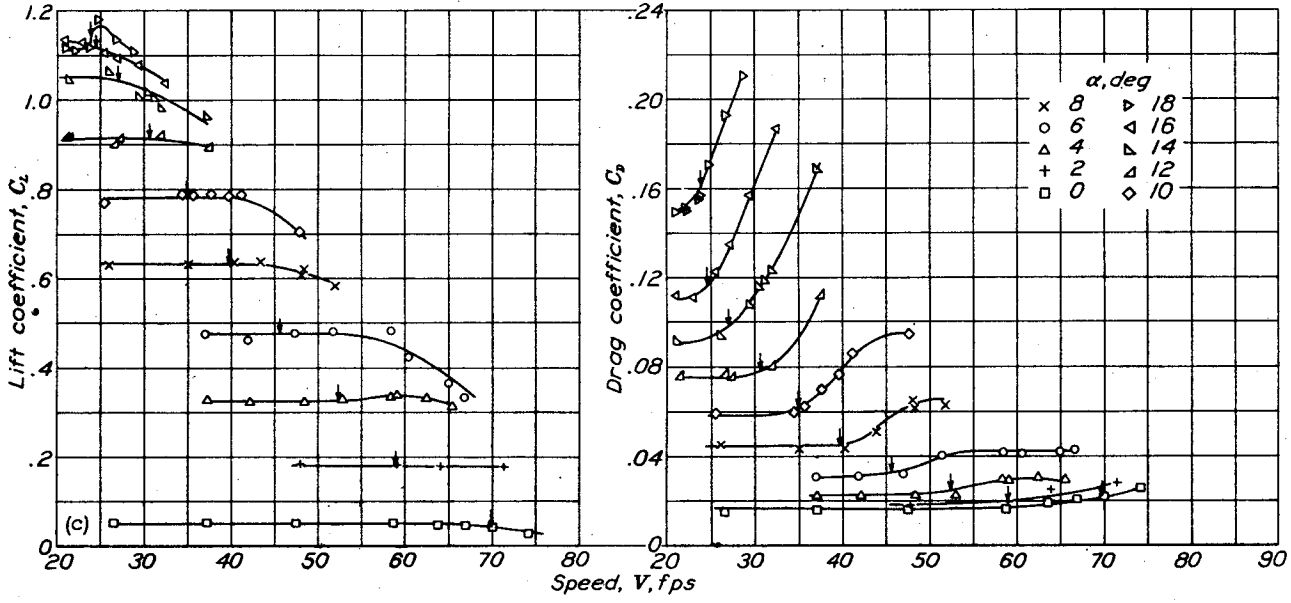

(d) d_o, 5c; t, 58.5°F; k, 1.49

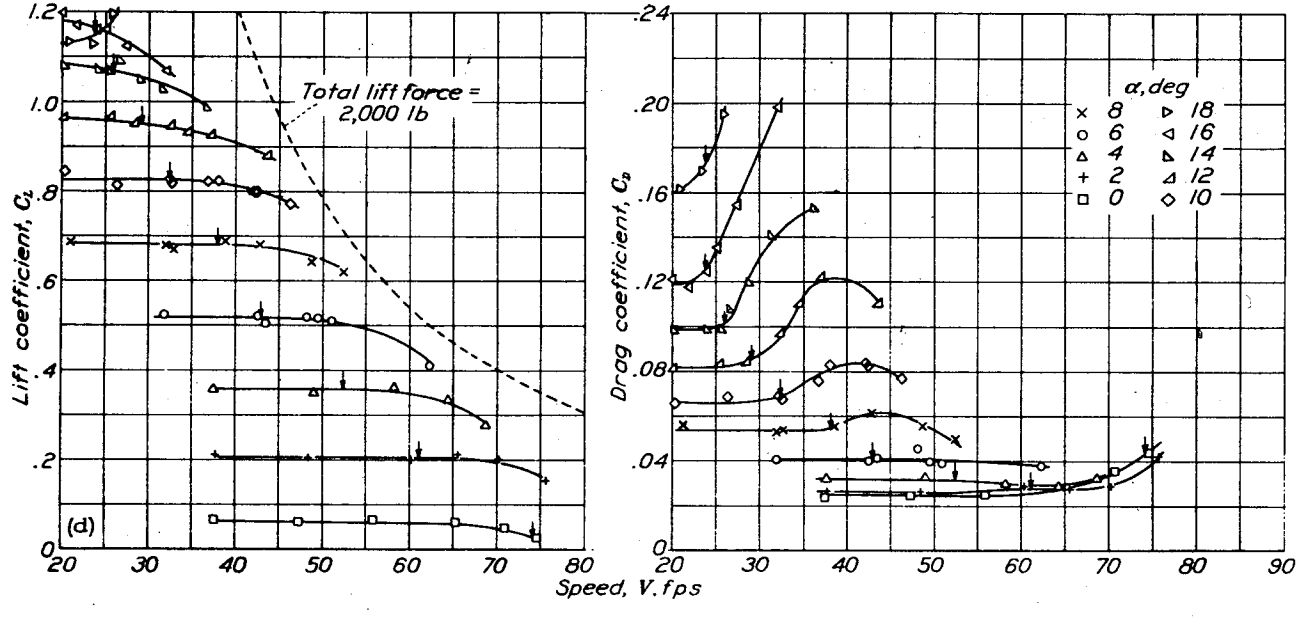

Figure 3.- Concluded.

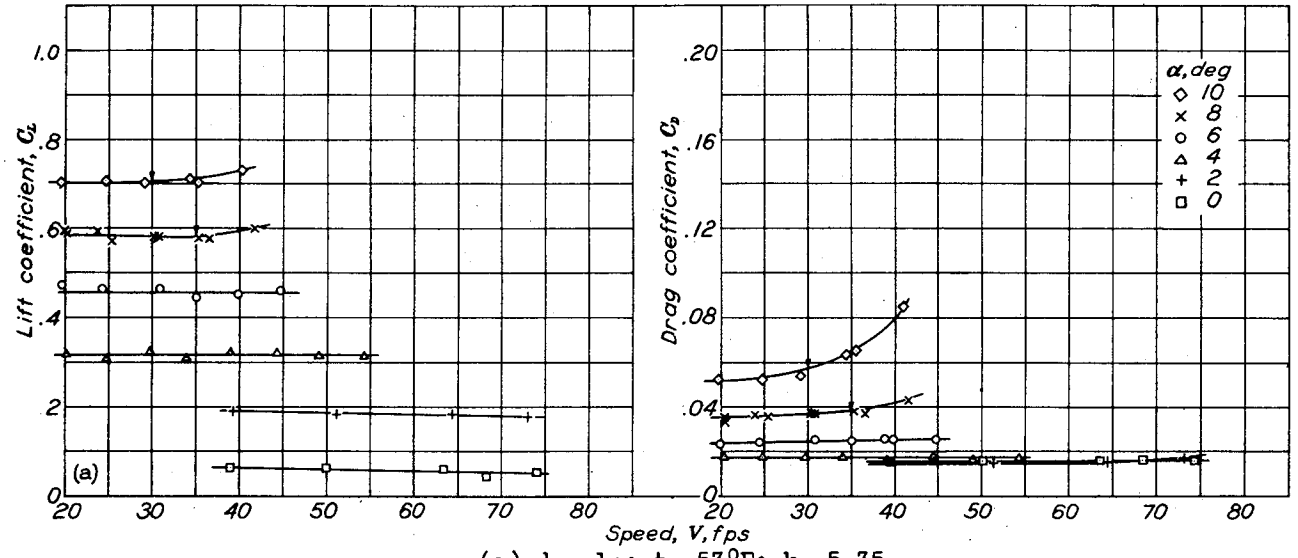

(a) d_o, 1c; t, 53°F; k, 5.35

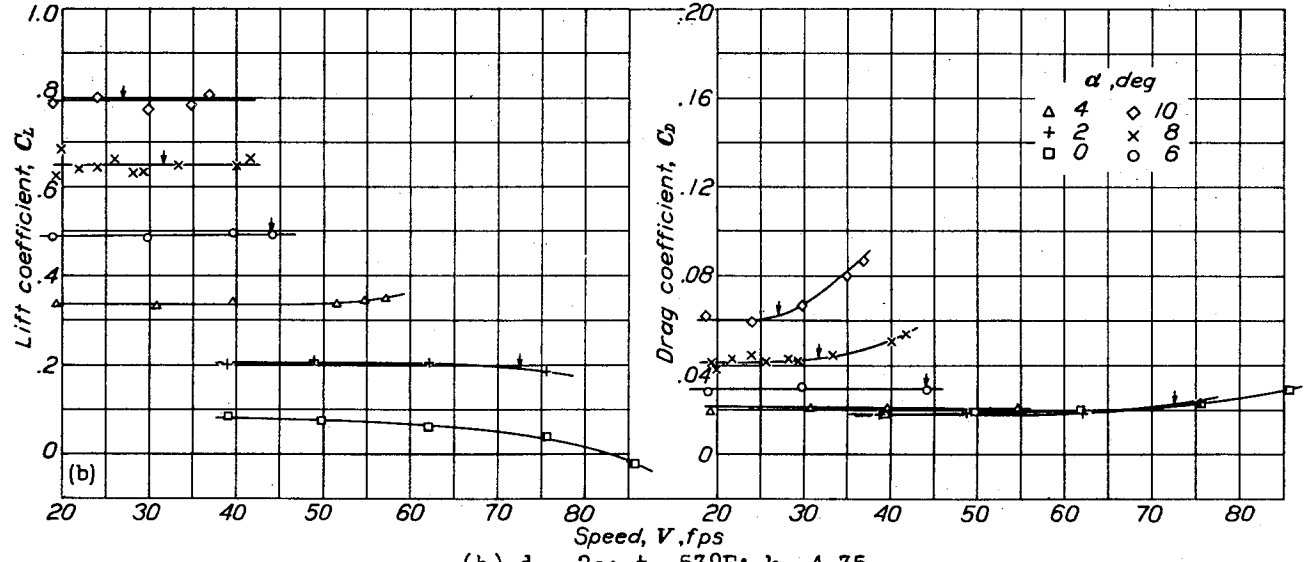

(b) d_o, 2c; t, 53°F; k, 4.35

Figure 4a,b.- NACA 23006-33 hydrofoil. Variation of C_L and C_D with V.

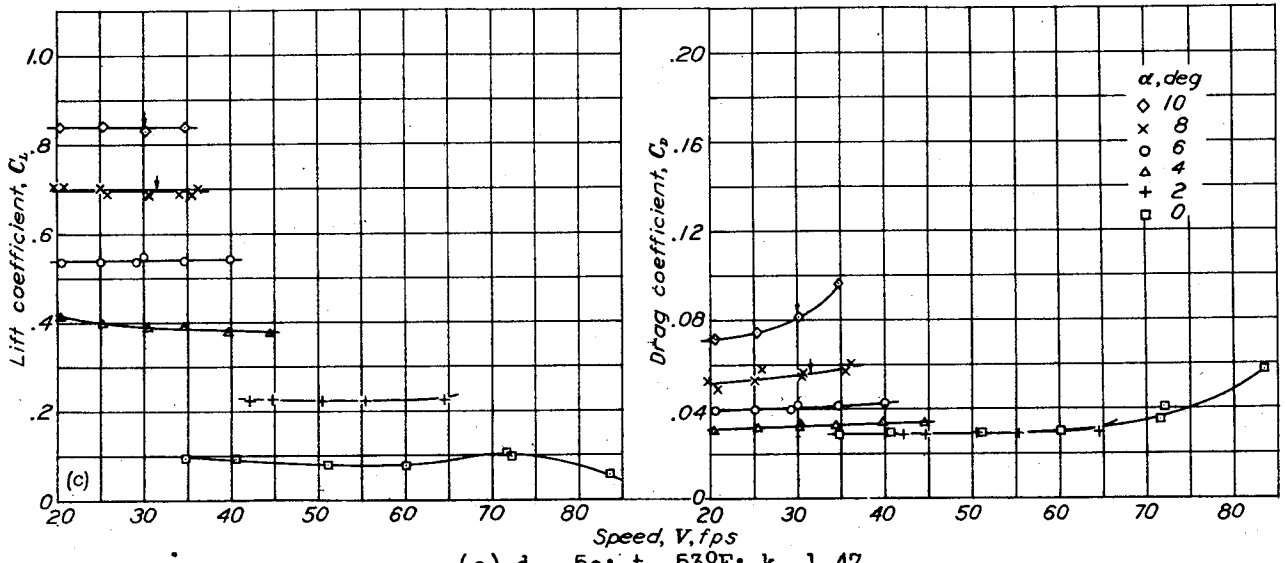

(c) d_o, 5c; t, 53°F; k, 1.47

Figure 4c.- NACA 23006-33 hydrofoil. Variation of C_L and C_D with V.

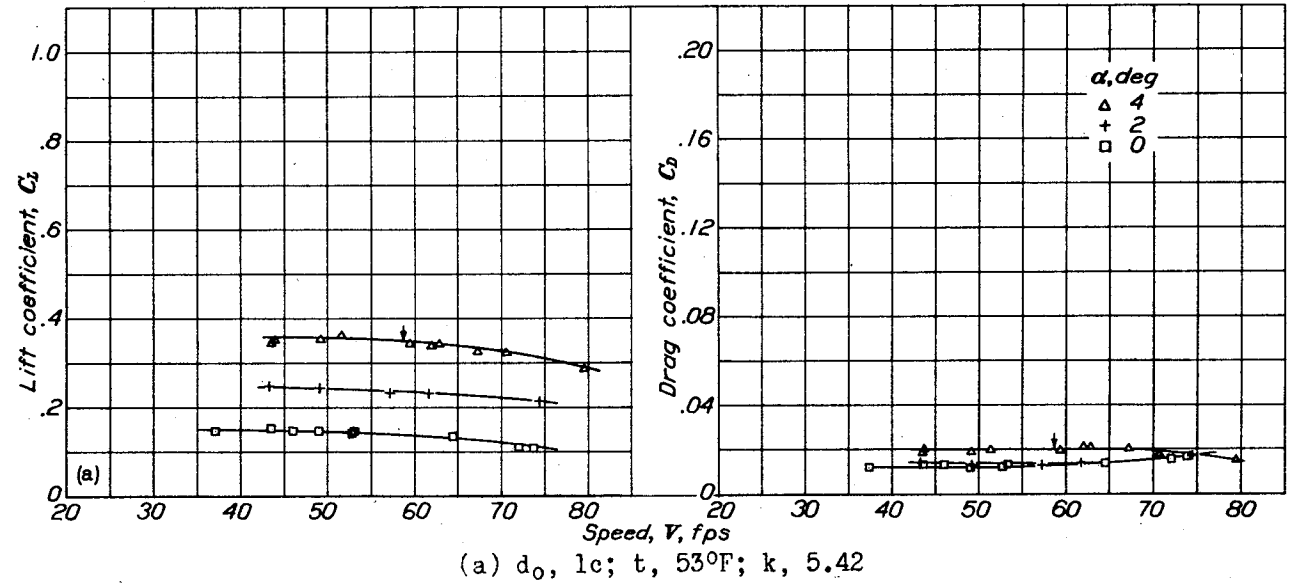

(a) d_o, 1c; t, 53°F; k, 5.42

Figure 5a.- NACA 25B09-46 hydrofoil. Variation of C_L and C_D with V.

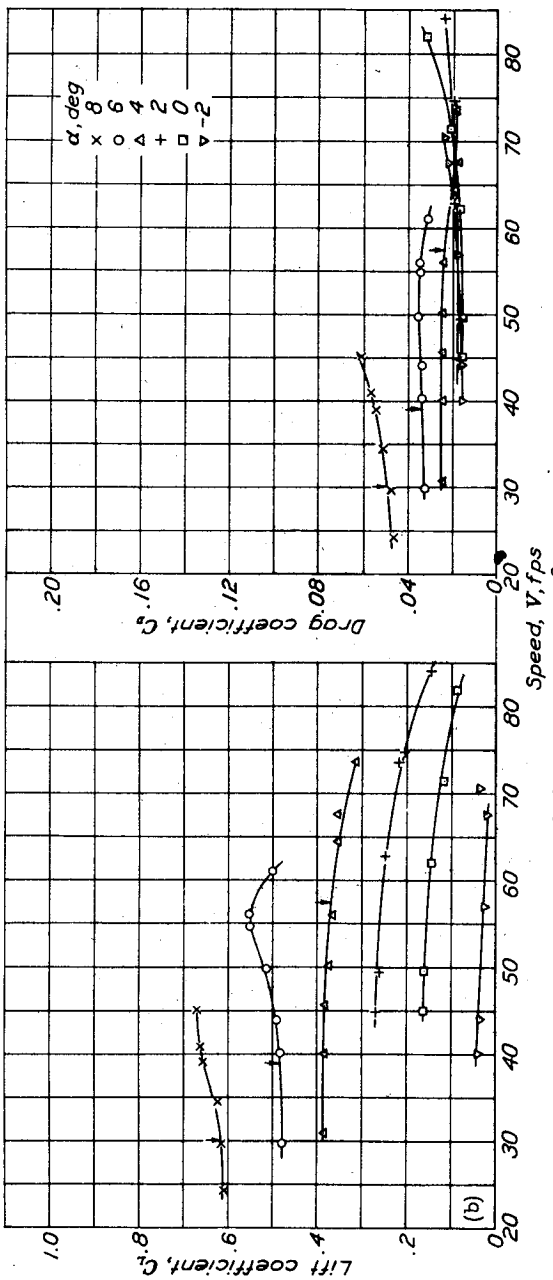

(b) d_o, 2c; t, 53°F; k, 4.42

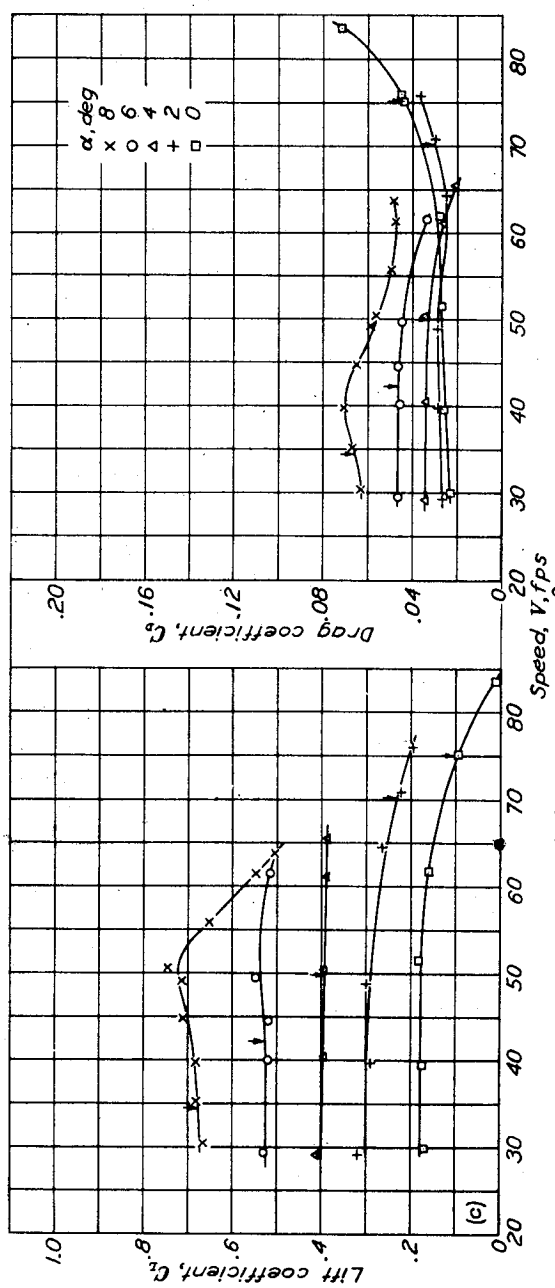

(c) d_o, 5c; t, 53°F; k, 1.42

Figure 5b,c.- NACA 25B09-46 hydrofoil. Variation of C_L and C_D with V.

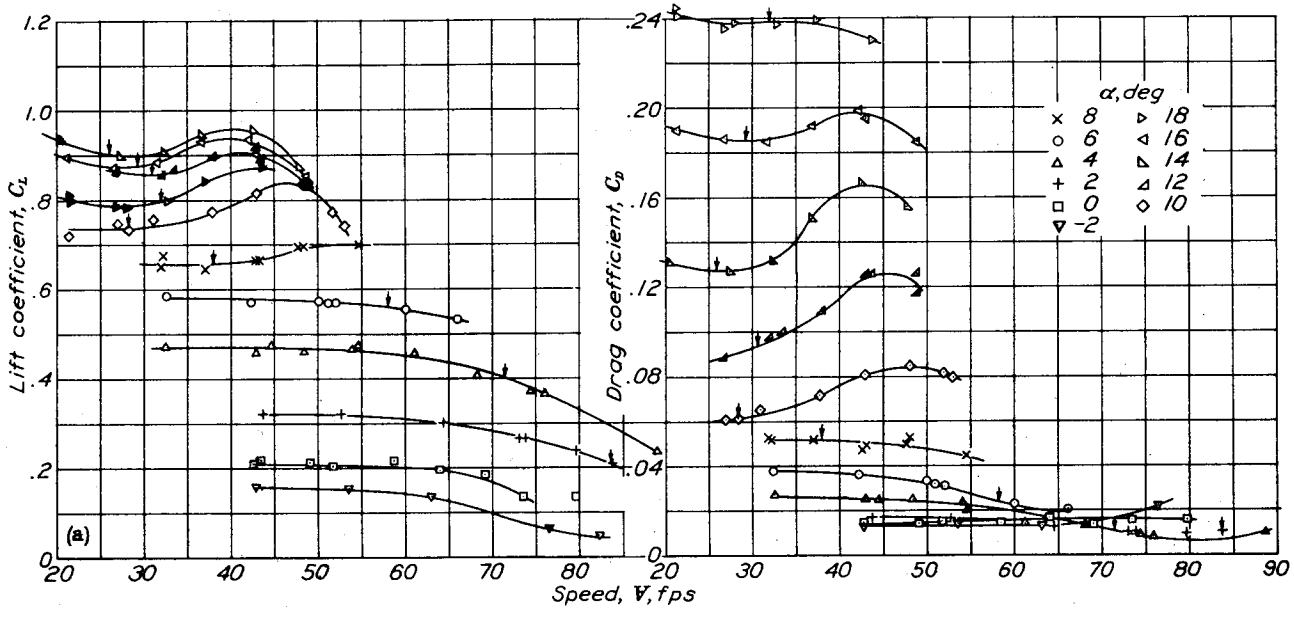

(a) d_o, 1c; t, 57.5°F; k, 5.41

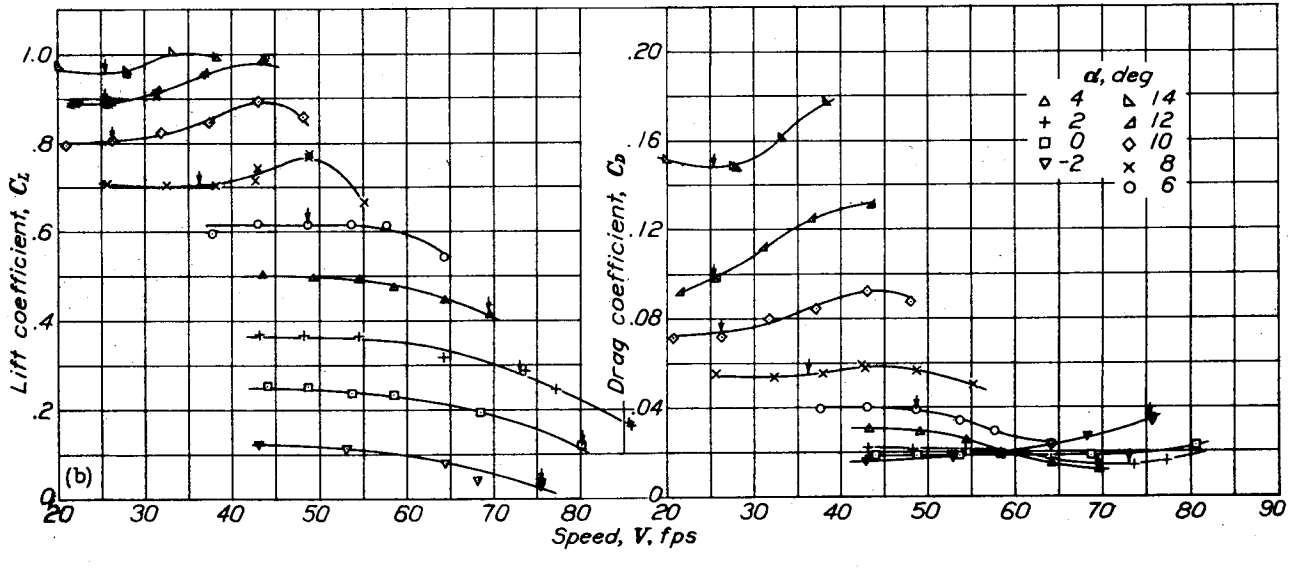

(b) d_o, 2c; t, 54.5°F; k, 4.50

Figure 6a,b.- NACA 16-509 hydrofoil. Variation of C_L and C_D with V.

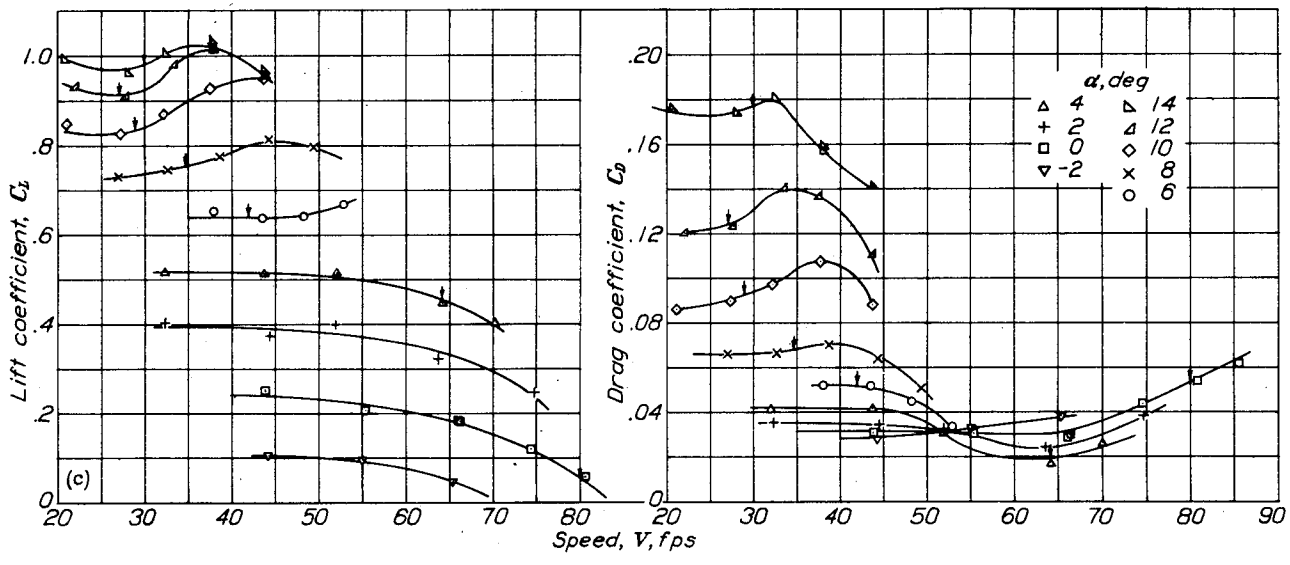

(c) d_o, 5c; t, 54.5°F; k, 1.51

Figure 6c.- NACA 16-509 hydrofoil. Variation of C_L and C_D with V.

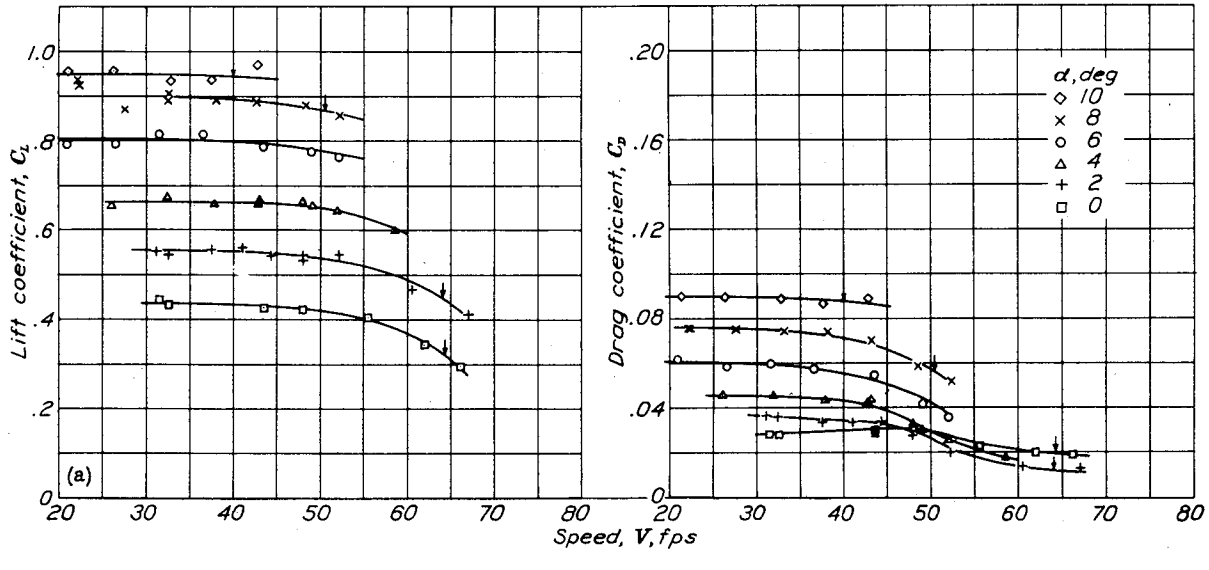

(a) d_o, 1c; t, 53°F; k, 5.38

Figure 7a.- NACA 16-1009 hydrofoil. Variation of C_L and C_D with V.

(b) d_0, 2c; t, 53°F; k, 4.52

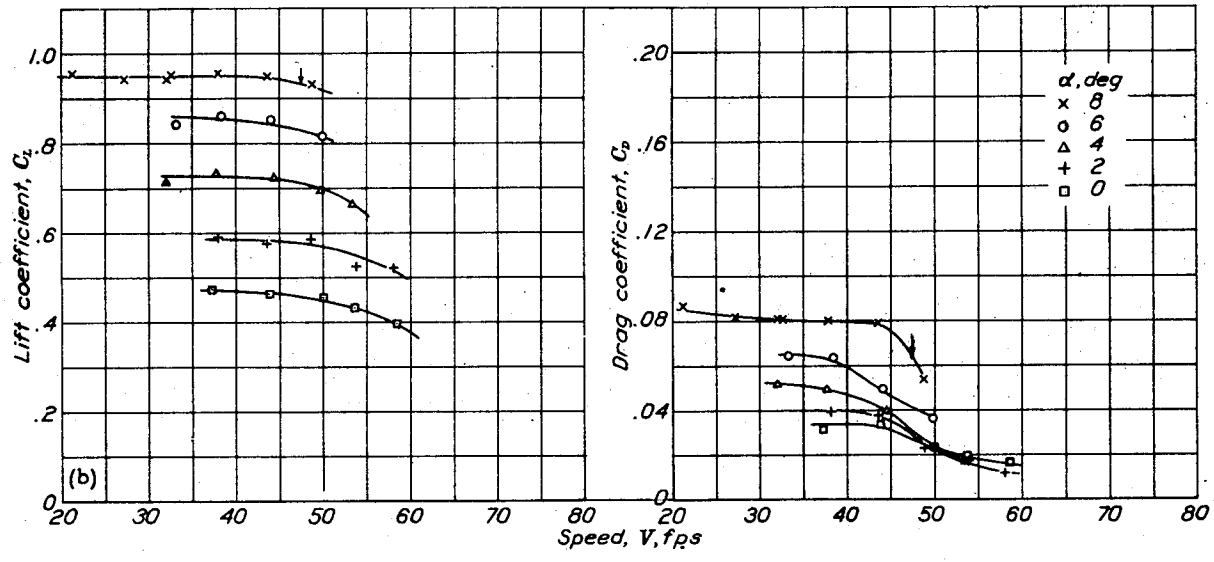

(c) d_0, 5c; t, 53°F; k, 1.51

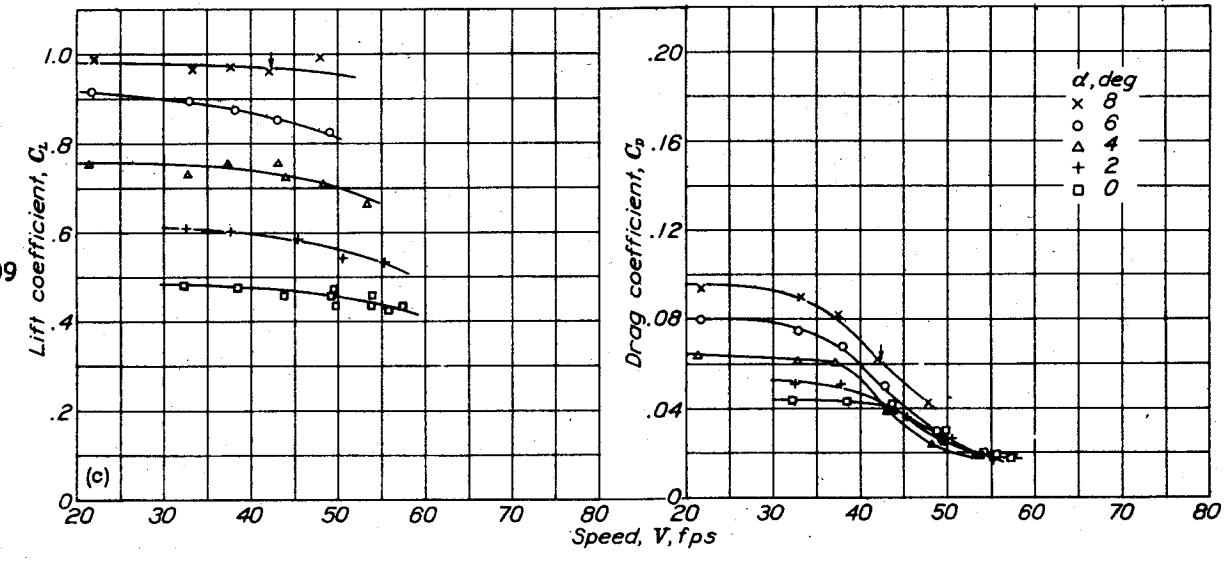

Figure 7b,c.- NACA 16-1009 hydrofoil. Variation of C_L and C_D with V.

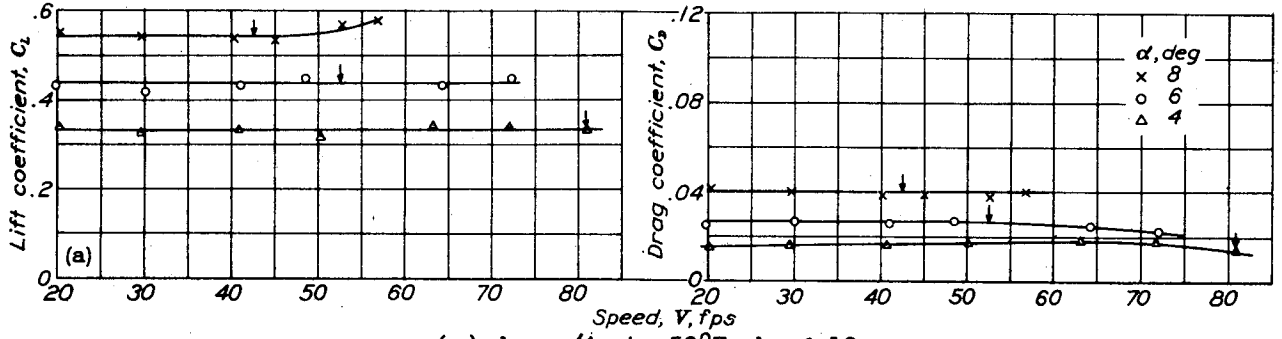

(a) d_o, c/4; t, 52°F; k, 6.19

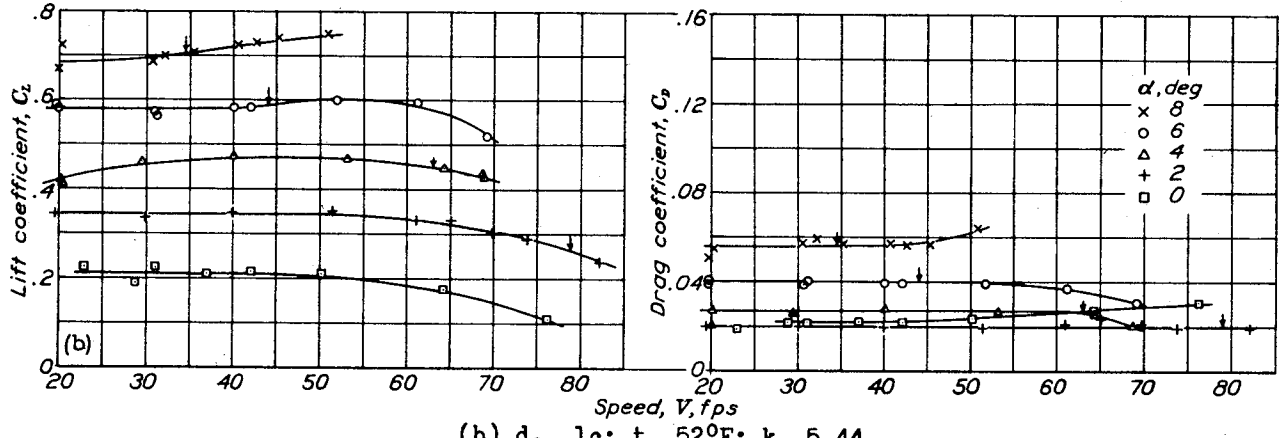

(b) d_o, 1c; t, 52°F; k, 5.44

Figure 8a to d.- Guidoni hydrofoil. Variation of C_L and C_D with V.

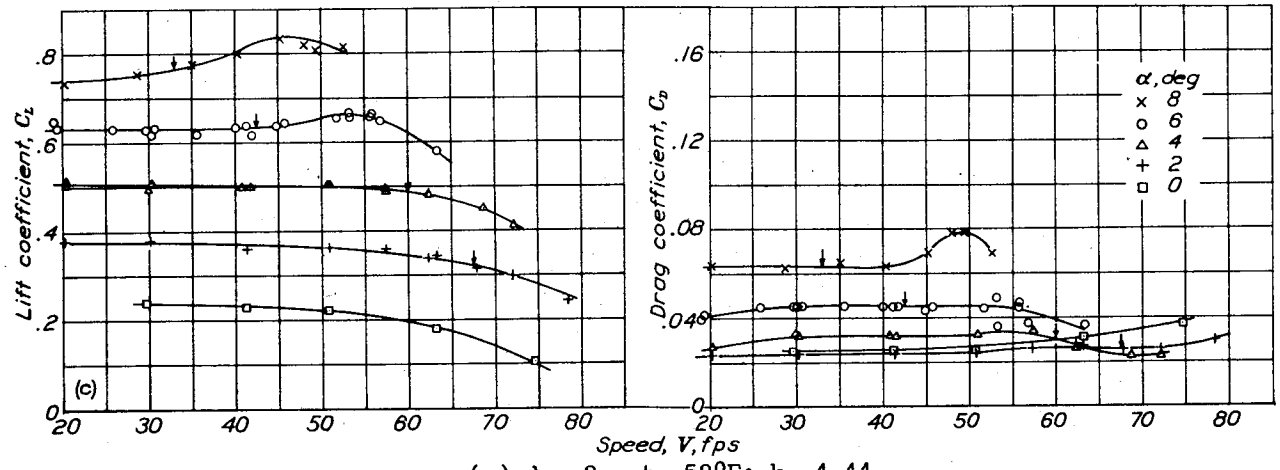

(c) d_o, 2c; t, 52°F; k, 4.44

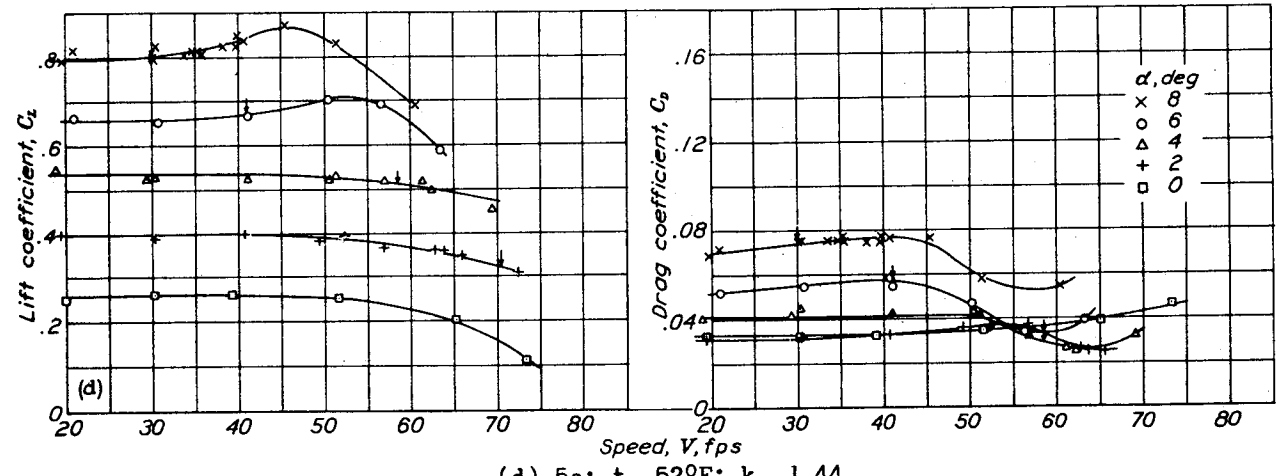

(d) 5c; t, 52°F; k, 1.44

Figure 8.- Concluded.

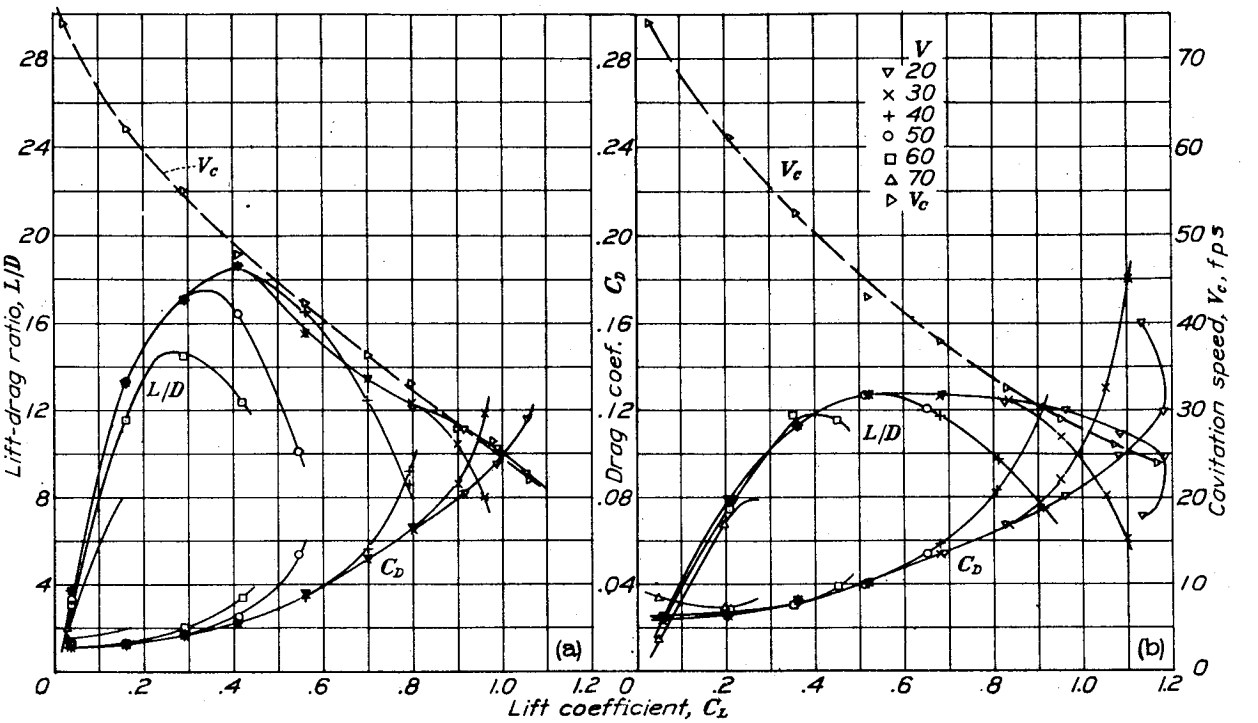

(a) d_o, 1c (b) d_o, 5c

Figure 9a,b.- NACA 23012 hydrofoil. Variation of C_D, L/D, and V_C with C_L.

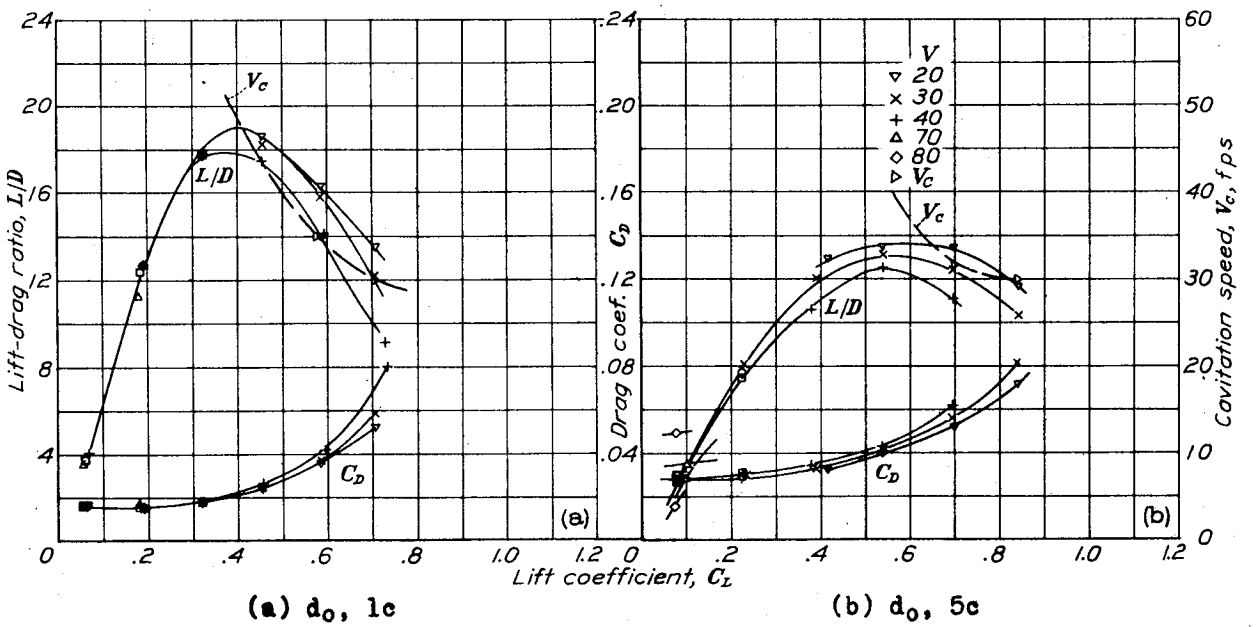

(a) d_o, 1c (b) d_o, 5c

Figure 10a,b.- NACA 23006-33 hydrofoil. Variation of C_D, L/D, and V_C with C_L.

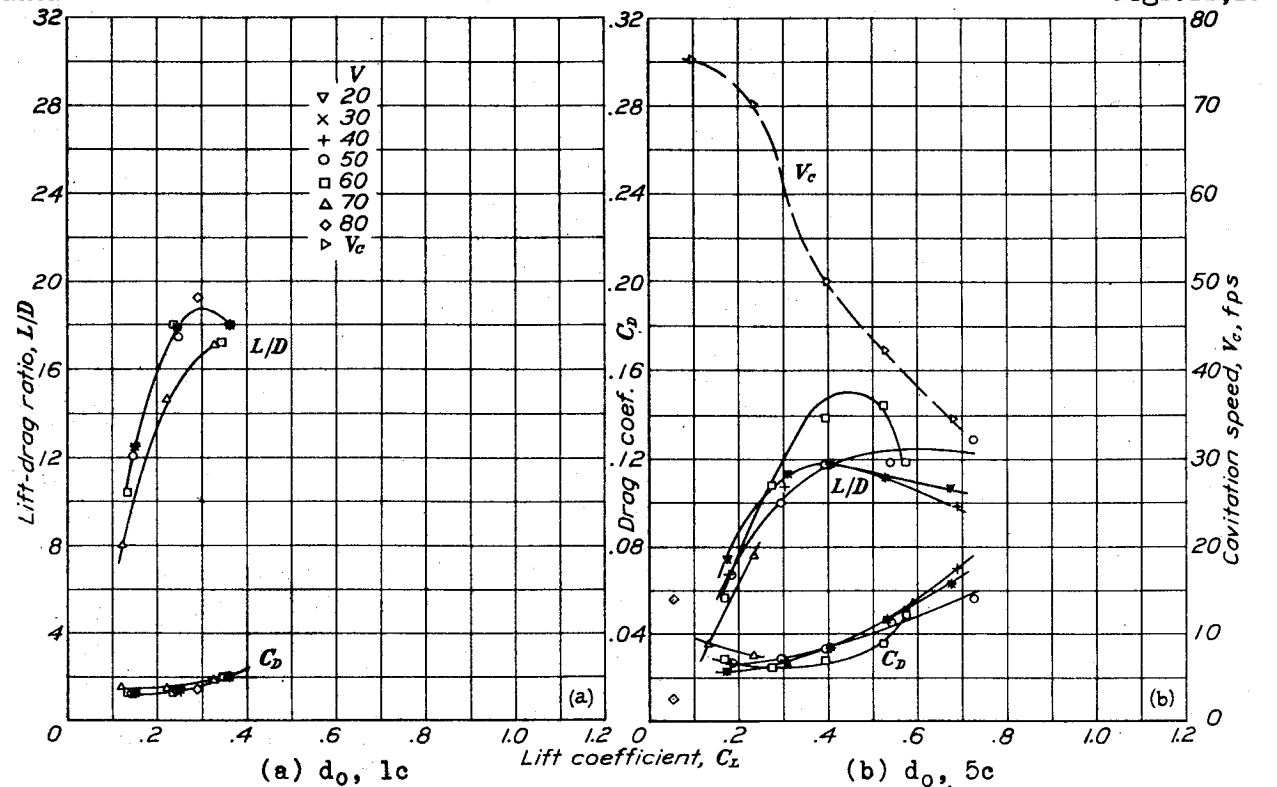

(a) d_o, 1c (b) d_o, 5c

Figure 11a,b.- NACA 25B09-46 hydrofoil. Variation of C_D, L/D, and V_C with C_L.

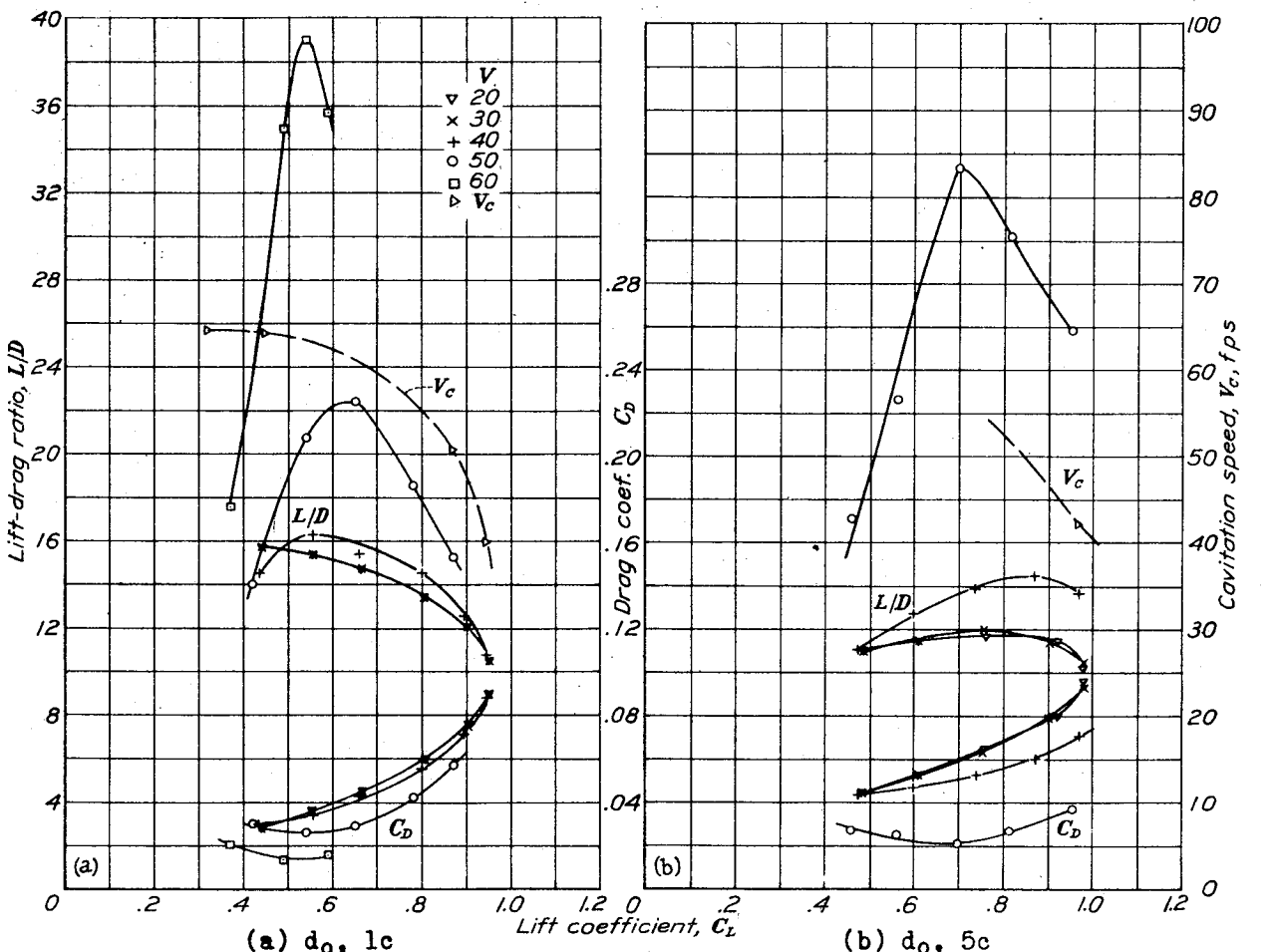

(a) d_o, 1c (b) d_o, 5c

Figure 13a,b.- NACA 16-1009 hydrofoil. Variation of C_D, L/D, and V_C with C_L.

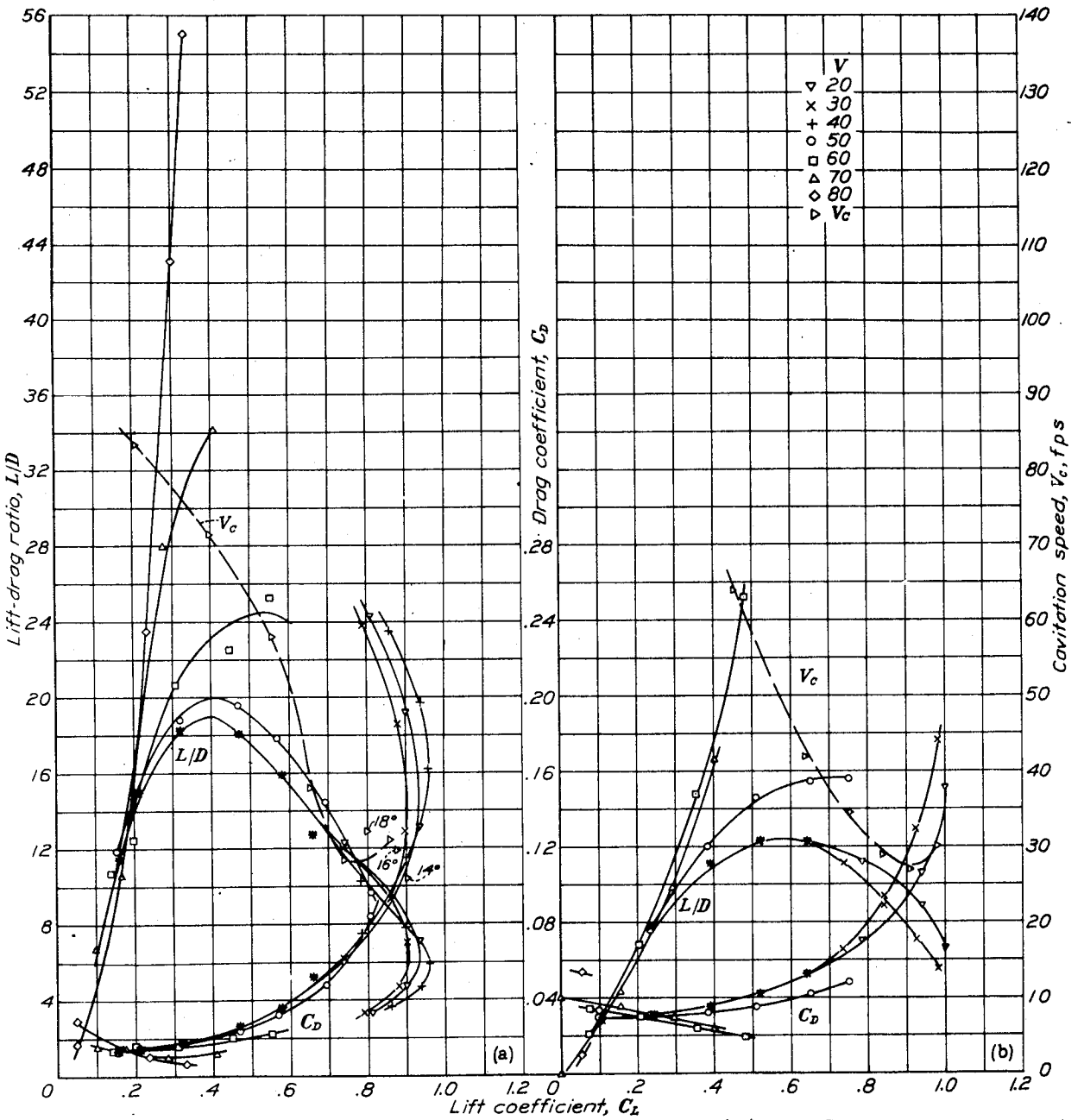

(a) d_o, 1c (b) d_o, 5c

Figure 12.- NACA 16-509 hydrofoil. Variation of C_D, L/D, and V_C with C_L.

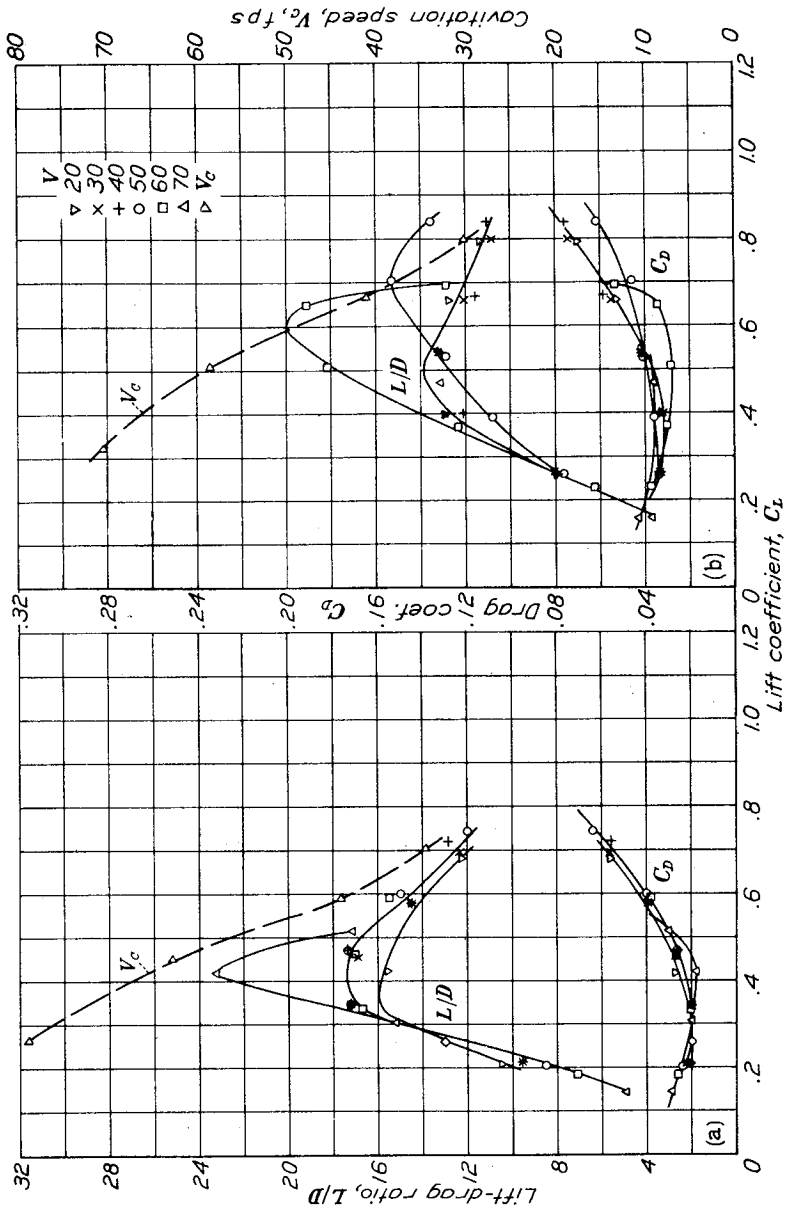

(a) d_o, 1c (b) d_o, 5c

Figure 14a,b.- Guidoni hydrofoil. Variation of C_D, L/D, and V_C with C_L.

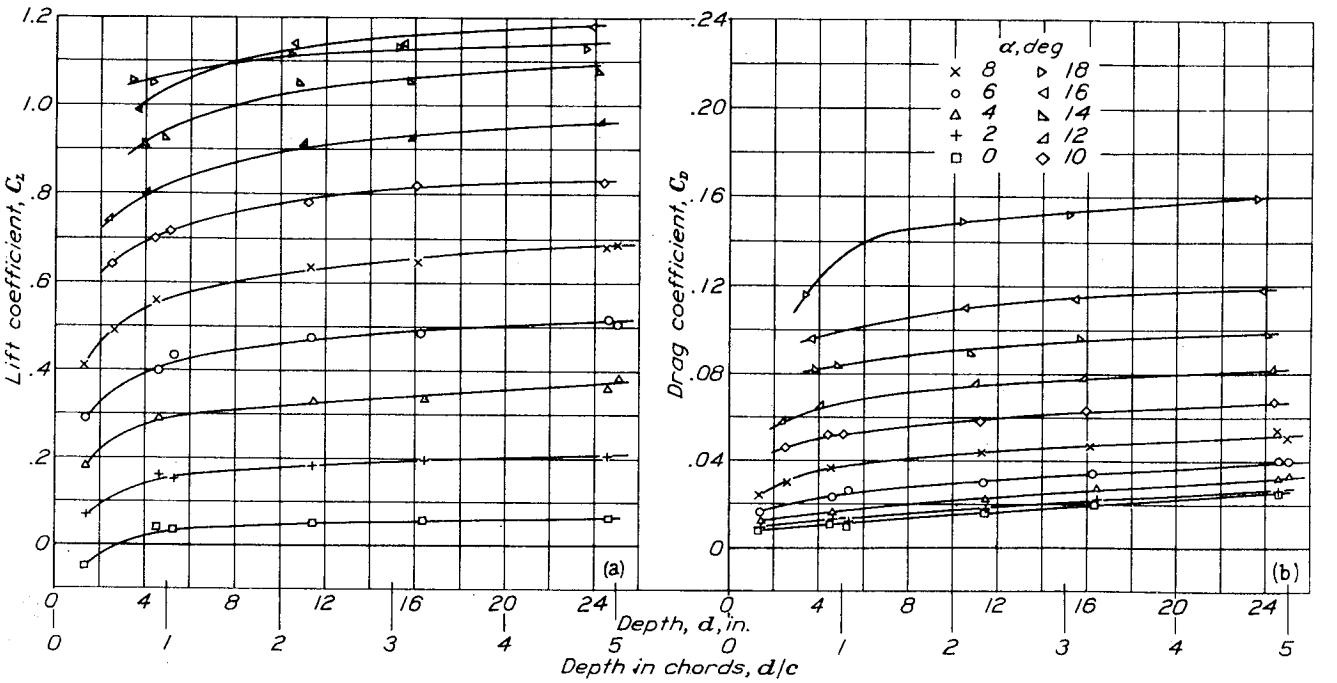

Figure 15.- NACA 23012 hydrofoil. Effect of depth on C_L and C_D.

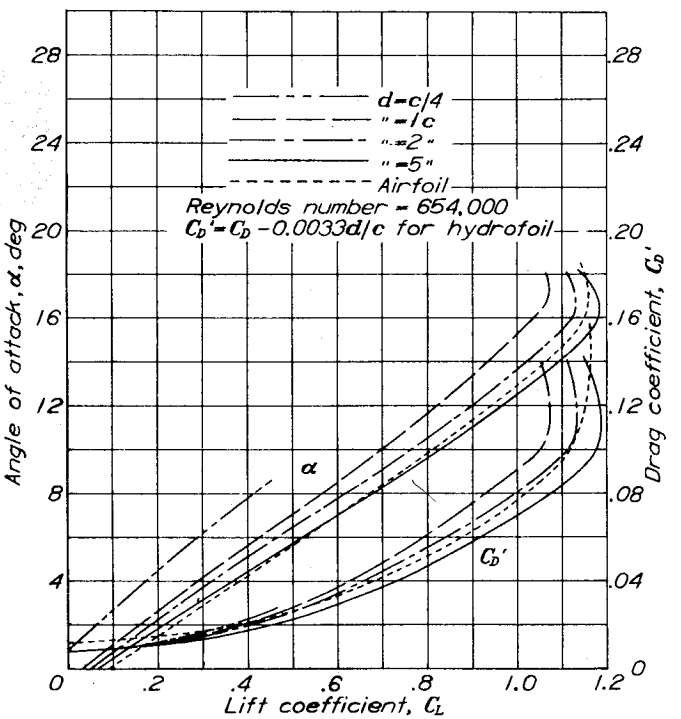

Figure 16.- Comparison of characteristics of NACA 23012 hydrofoil with those of a similar NACA 23012 airfoil.

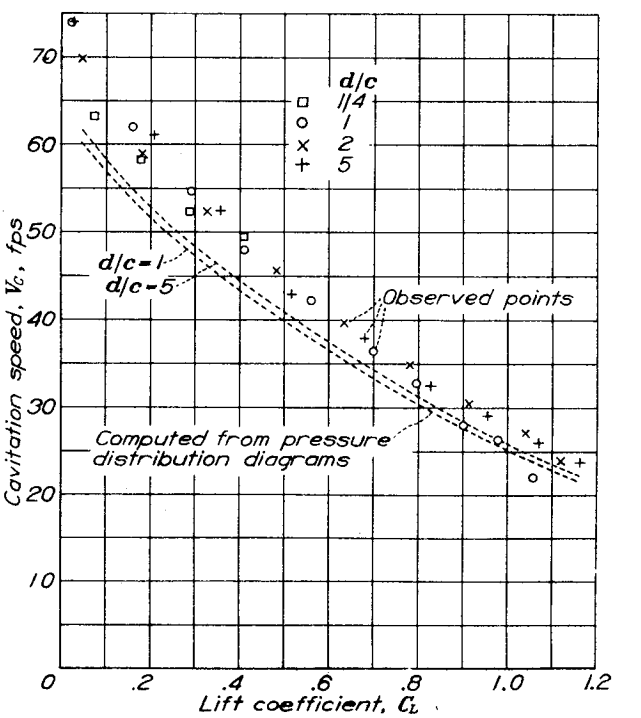

Figure 17.- Comparison of observed with computed cavitation speeds for NACA 23012 hydrofoil.

NACA

Fig. 18a

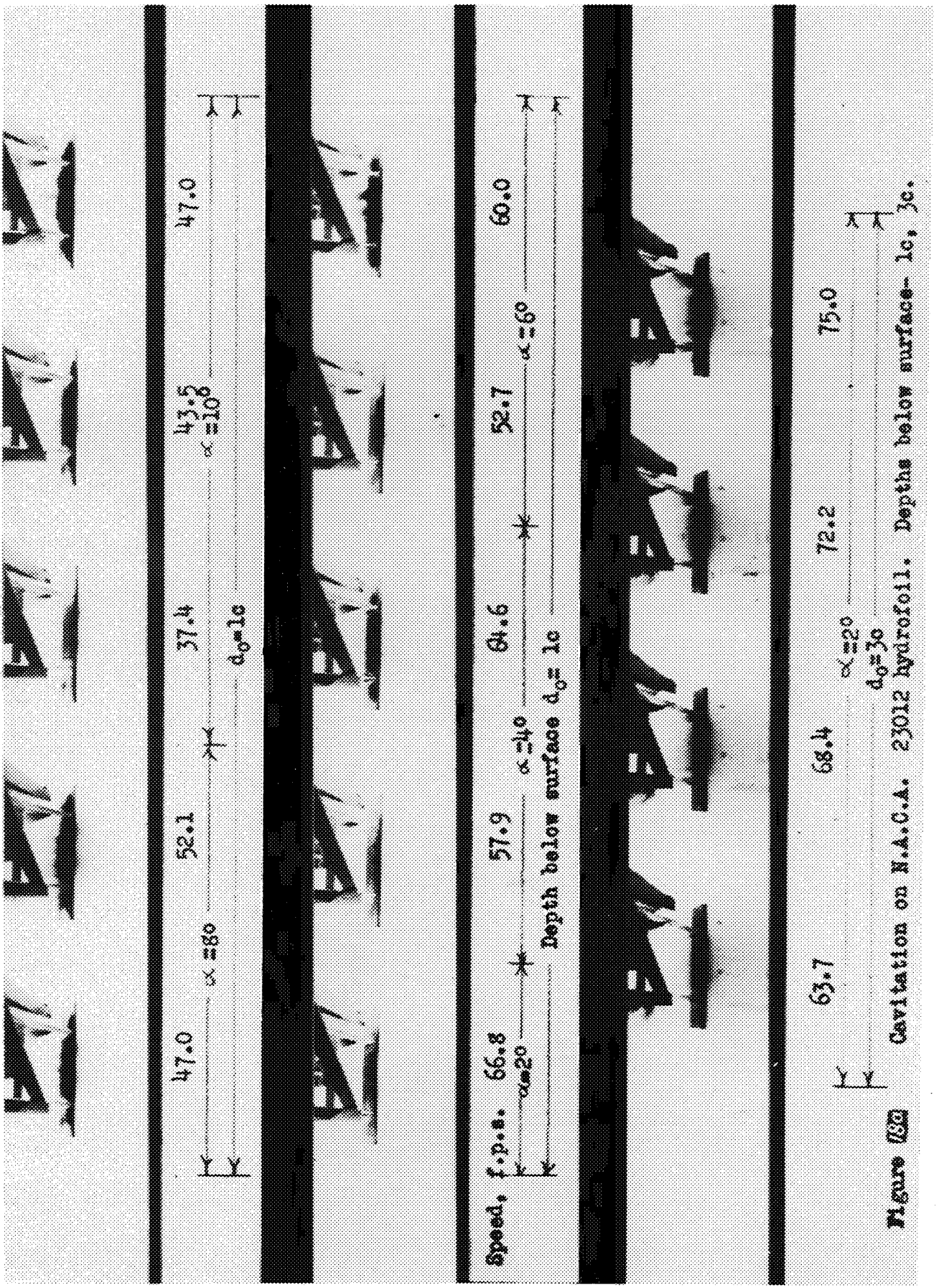

Figure 18a Cavitation on N.A.C.A. 23012 hydrofoil. Depths below surface- 1c, 3c.

NACA

Fig. 18b

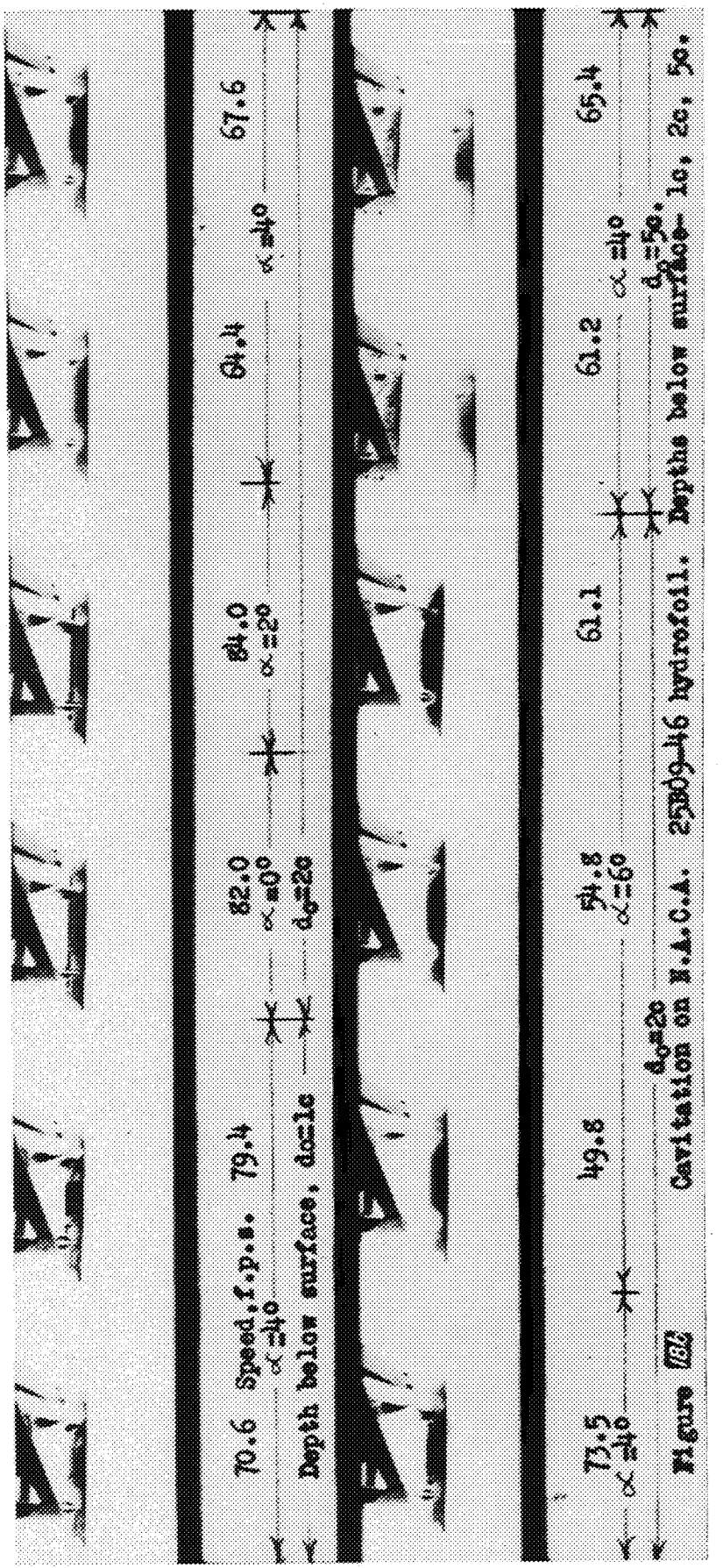

Figure 18 Cavitation on N.A.C.A. 2309-46 hydrofoil. Depths below surface= 1c, 2c, 5c.

NACA

Fig. 18c

Figure 18. Cavitation on N.A.C.A. 16-509 hydrofoil. Depths below surface- 1c, 2c, 5c.

NACA

Fig. 18d

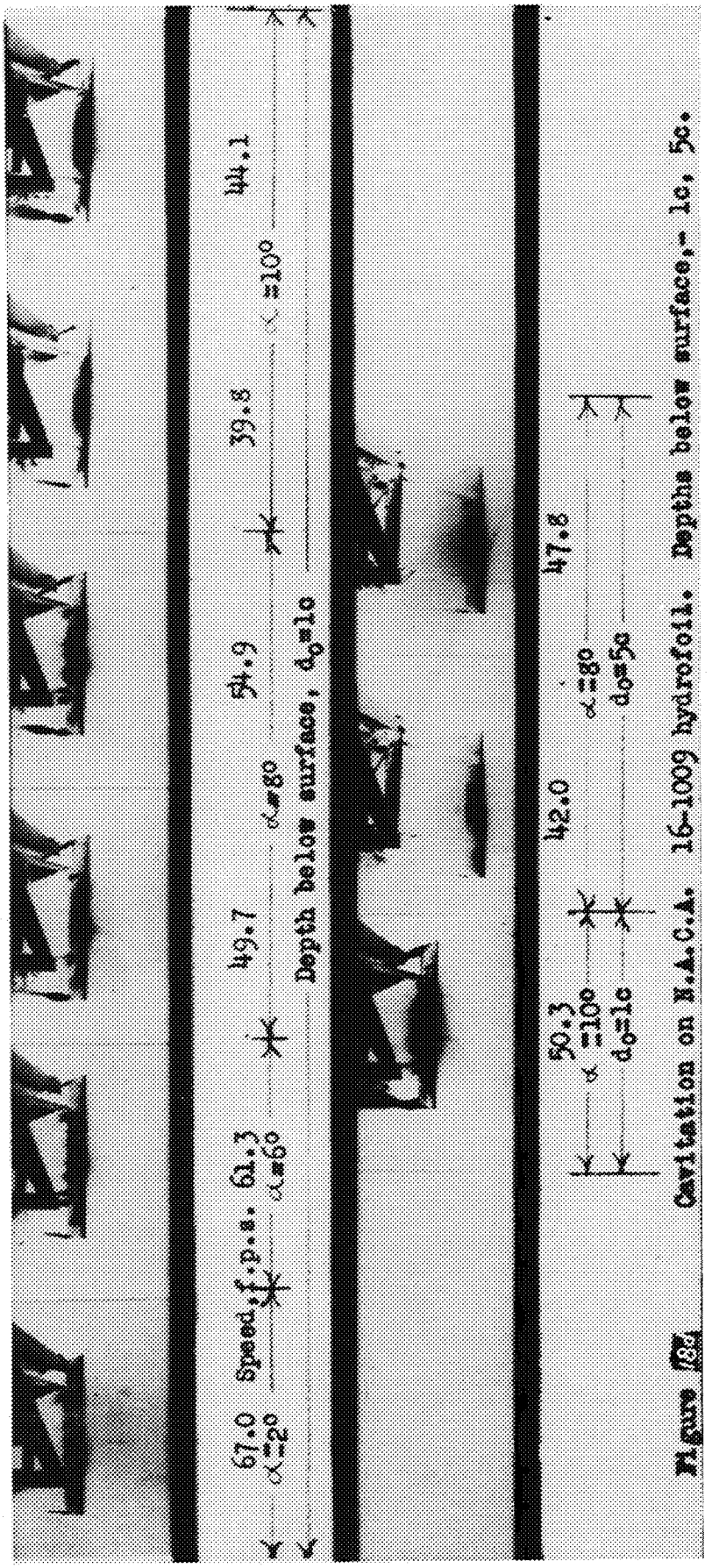

Figure 18d. Cavitation on N.A.C.A. 16-1009 hydrofoil. Depths below surface,- 1c, 5c.

NACA

Fig. 18e

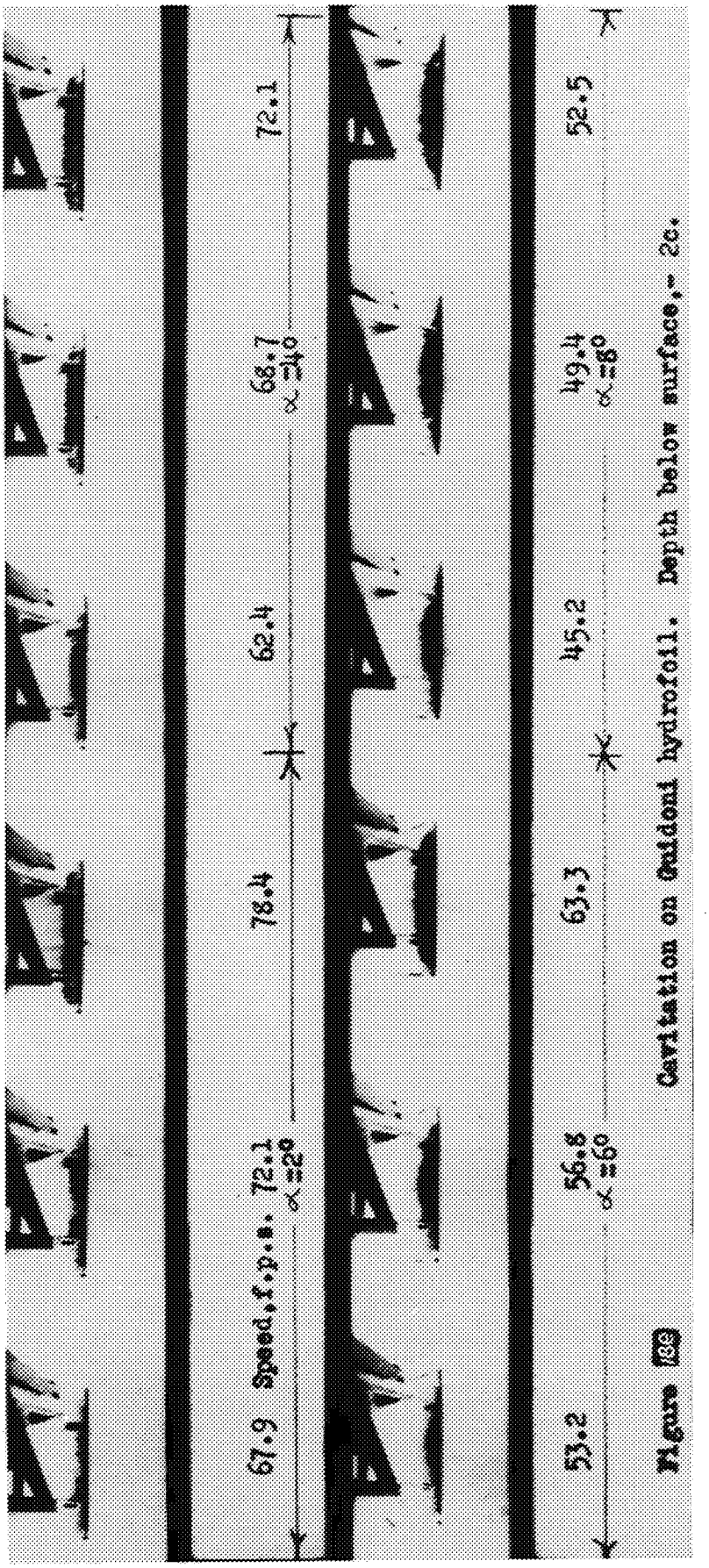

Figure [illegible] Cavitation on Guidoni hydrofoil. Depth below surface, ~ 2c.